

Spin - dependent Transport Through Carbon Nanotubes

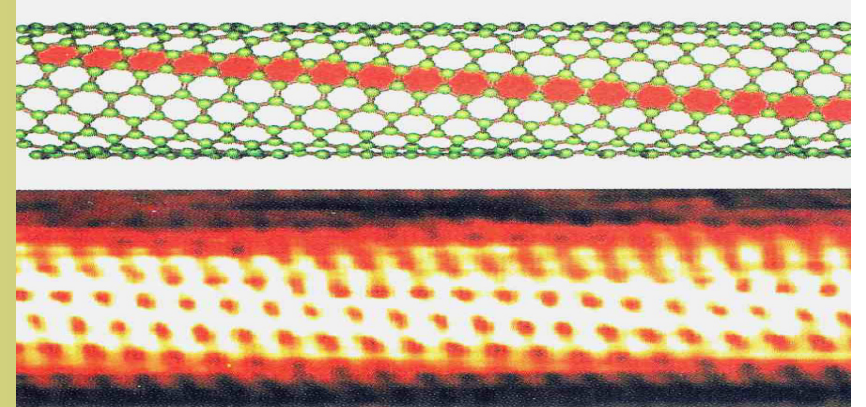
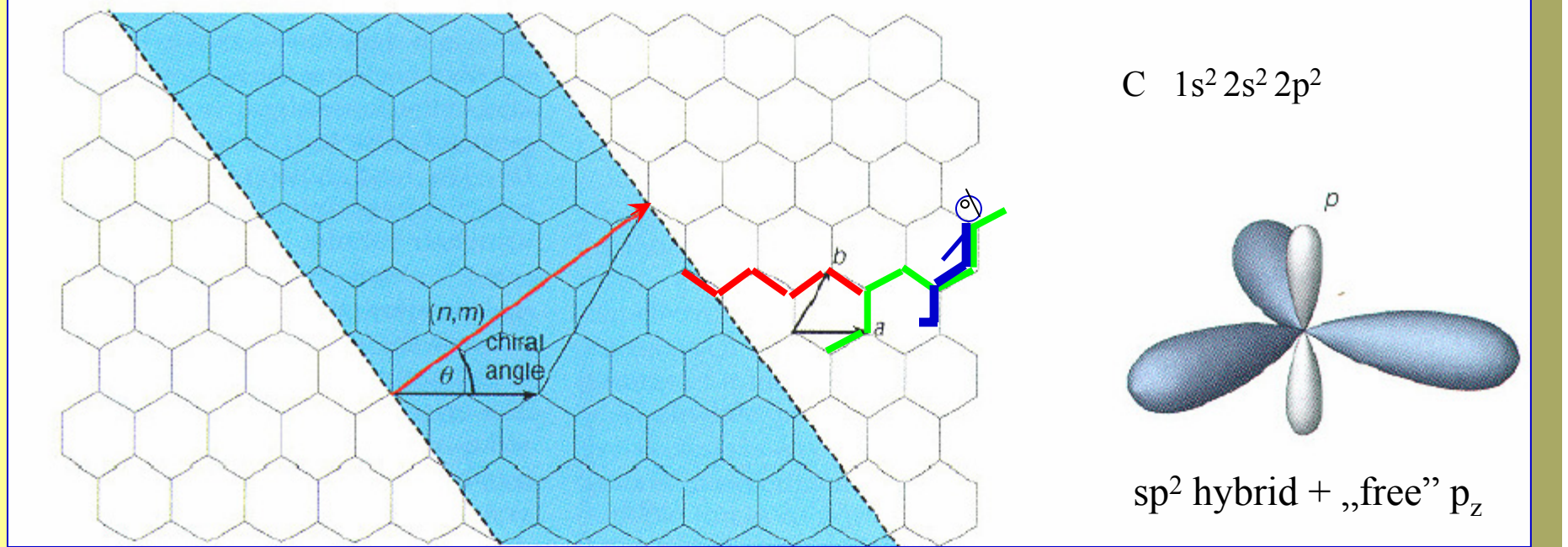
S. Krompiewski



*Institute of Molecular Physics, Polish Academy of Sciences,
M. Smoluchowskiego 17, 60-179 Poznań, Poland*

OUTLINE

1. Conductance through a molecule
(fundamentals).
2. Carbon nanotube as a confined quantum dot
(quasi - ballistic, Kondo and Coulomb
regimes).
3. Giant and tunnel magnetoresistance (GMR,
TMR)



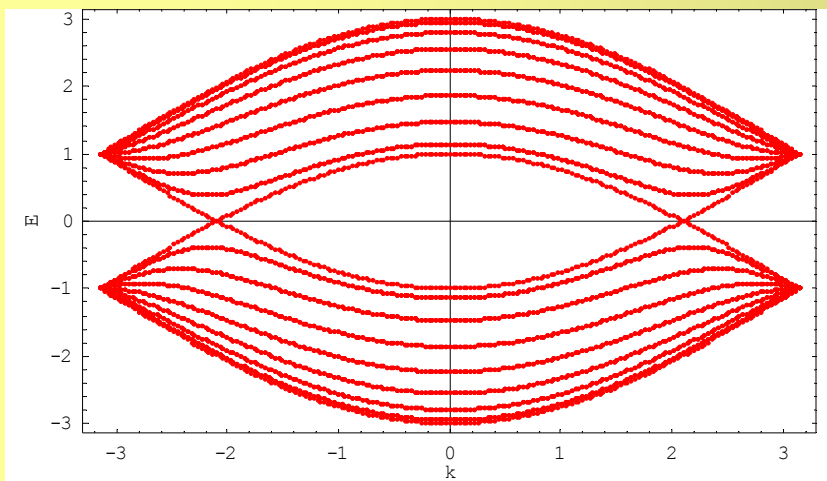
Metallic vs. semiconducting behaviour

$$n - m = 3 i, \quad (i = \text{integer})$$

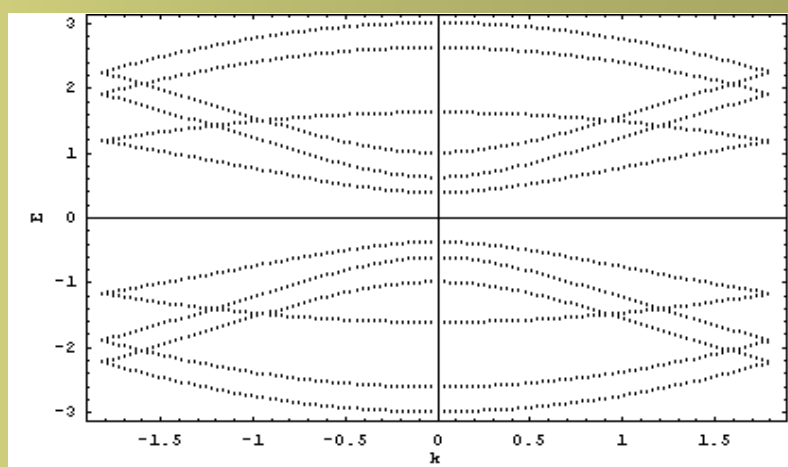
The wrapping vector $R = (n, m)$ on the graphite sheet (equals to the circumference of the nanotube) determines the chirality

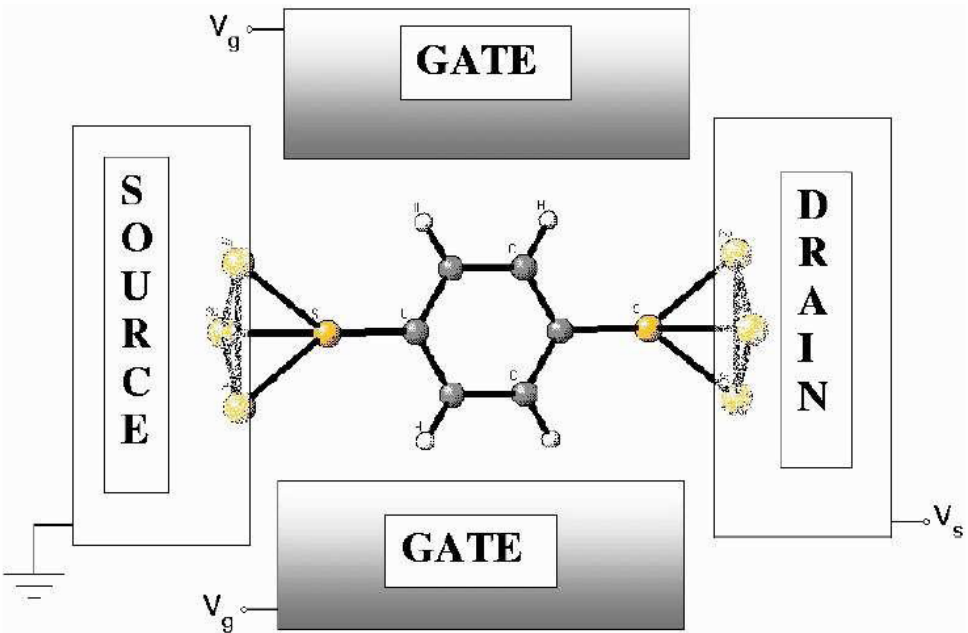
e.g.: $n = m$ ‘armchair’, $R = (n, 0)$ ‘zigzag’

Armchair (8,8)

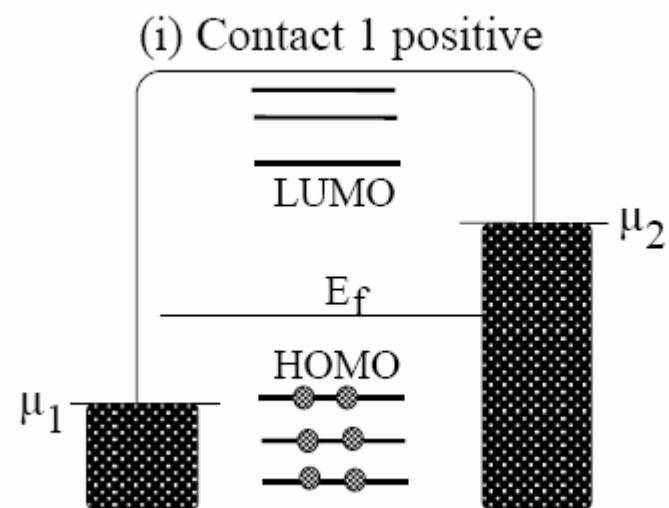


Zigzag (5,0)





Supriyo Datta et al.
Purdue University



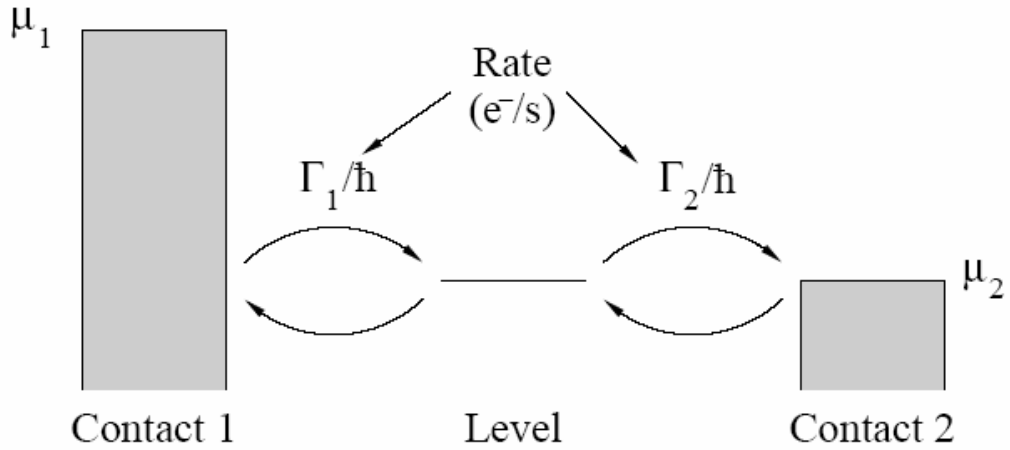


Illustration of the kinetic equation.

(Γ_i/\hbar tunnel rates)

$N_i = 2$ (for spin) $f(\varepsilon, \mu_i)$; $i = 1, 2$ (if the level were in equilibrium with contact i)

$$I_1 = (e \Gamma_1 / \hbar) (N_1 - N), \quad I_2 = (e \Gamma_2 / \hbar) (N - N_2)$$

$$I_1 = I_2 \quad (\text{steady state})$$

$$N = 2 [\Gamma_1 f(\varepsilon, \mu_1) + \Gamma_2 f(\varepsilon, \mu_2)] / (\Gamma_1 + \Gamma_2)$$

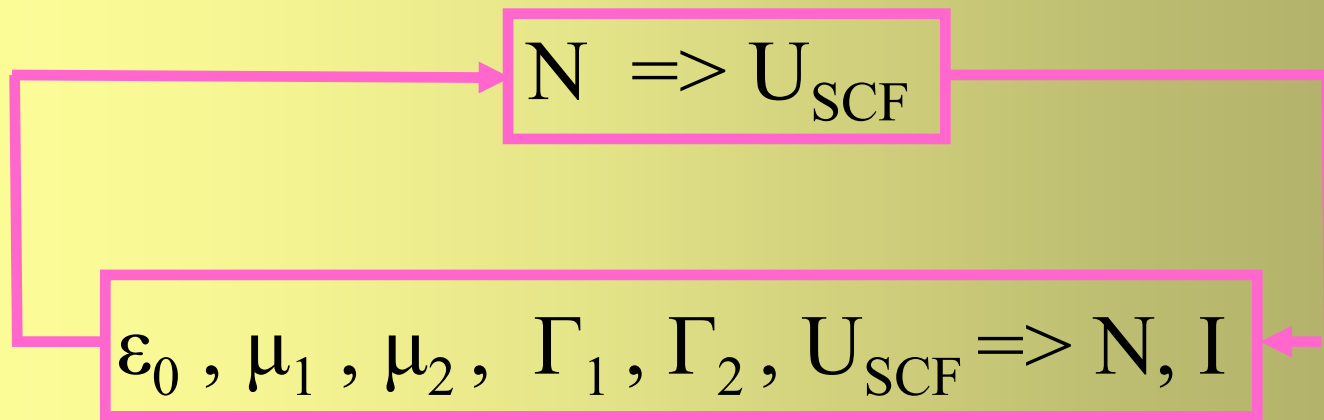
$$I = (2e/\hbar) [\Gamma_1 \Gamma_2 / (\Gamma_1 + \Gamma_2)] [f(\varepsilon, \mu_1) - f(\varepsilon, \mu_2)]$$

$$V = (\mu_2 - \mu_1) / |e|$$

Self-consistency to include charging

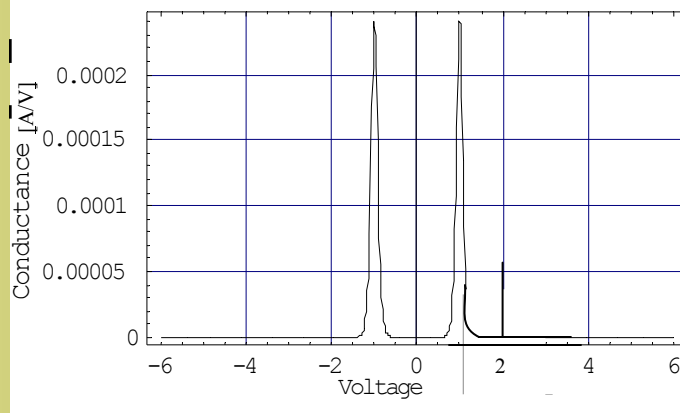
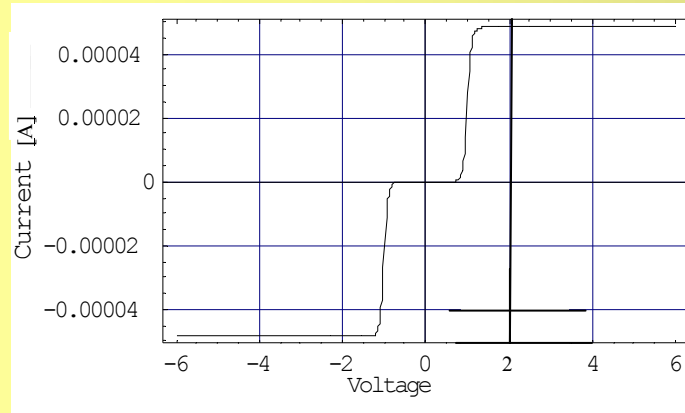
$$U_{SCF} = U [N - 2 f(\varepsilon_0, E_F)]$$

$$\varepsilon = \varepsilon_0 + U_{SCF}$$

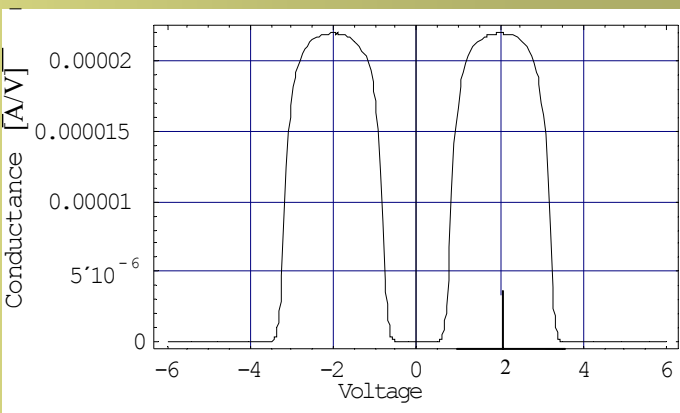
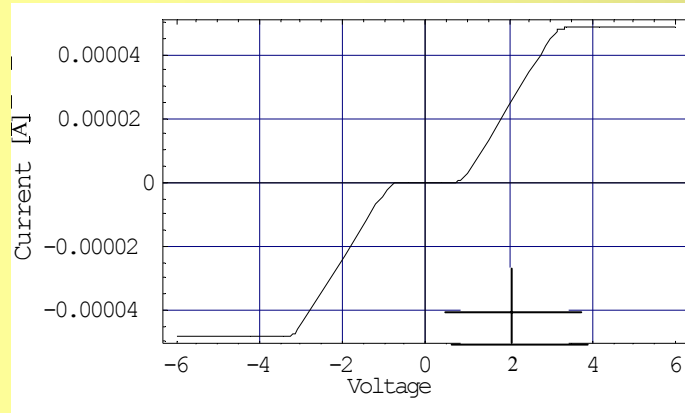


(Unrestricted model: $\varepsilon_\sigma = \varepsilon_0 + U [N_\sigma - f_0]$, $\sigma = \uparrow, \downarrow$)

e.g.: $E_F = -5$, $\varepsilon_0 = -5.5$, $\Gamma_1 = \Gamma_2 = 0.2$ (each in eV)



$U=0$



$U=1$

Further improvements and generalizations

- Broadening (Lorentzian)

$$D(E) = [\Gamma/(2\pi)] / [(E - \varepsilon)^2 + (\Gamma/2)^2]$$

- Non-equilibrium GF (NEGF)

$$\mathbf{G}(E) = (E \mathbf{1} - \mathbf{H} - \boldsymbol{\Sigma}_1 - \boldsymbol{\Sigma}_2)^{-1}$$

$$\boldsymbol{\Gamma}_{1,2} = i(\boldsymbol{\Sigma}_{1,2} - \boldsymbol{\Sigma}_{1,2}^+)$$

$$I = (2e/h) \int dE \operatorname{Tr} [\boldsymbol{\Gamma}_1 \mathbf{G} \boldsymbol{\Gamma}_2 \mathbf{G}^+] [f(E, \mu_1) - f(E, \mu_1)]$$

$$N = \operatorname{Tr}(\rho)$$

$$\rho = (1/\pi) \int dE [f(E, \mu_1) \mathbf{G} \boldsymbol{\Gamma}_1 \mathbf{G}^+ + f(E, \mu_2) \mathbf{G} \boldsymbol{\Gamma}_2 \mathbf{G}^+]$$

$$\boldsymbol{\Sigma}_i = \mathbf{V}_i \mathbf{g}^{\text{electrod}(i)} \mathbf{V}_i^+$$

Kinetic equation  NEGF

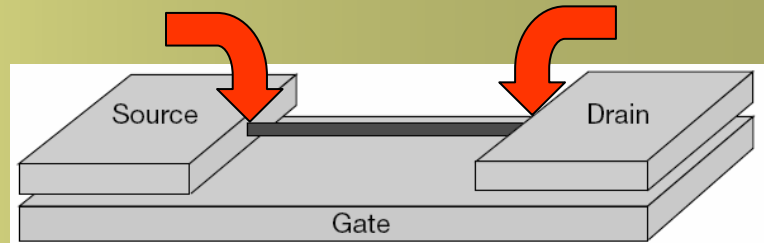
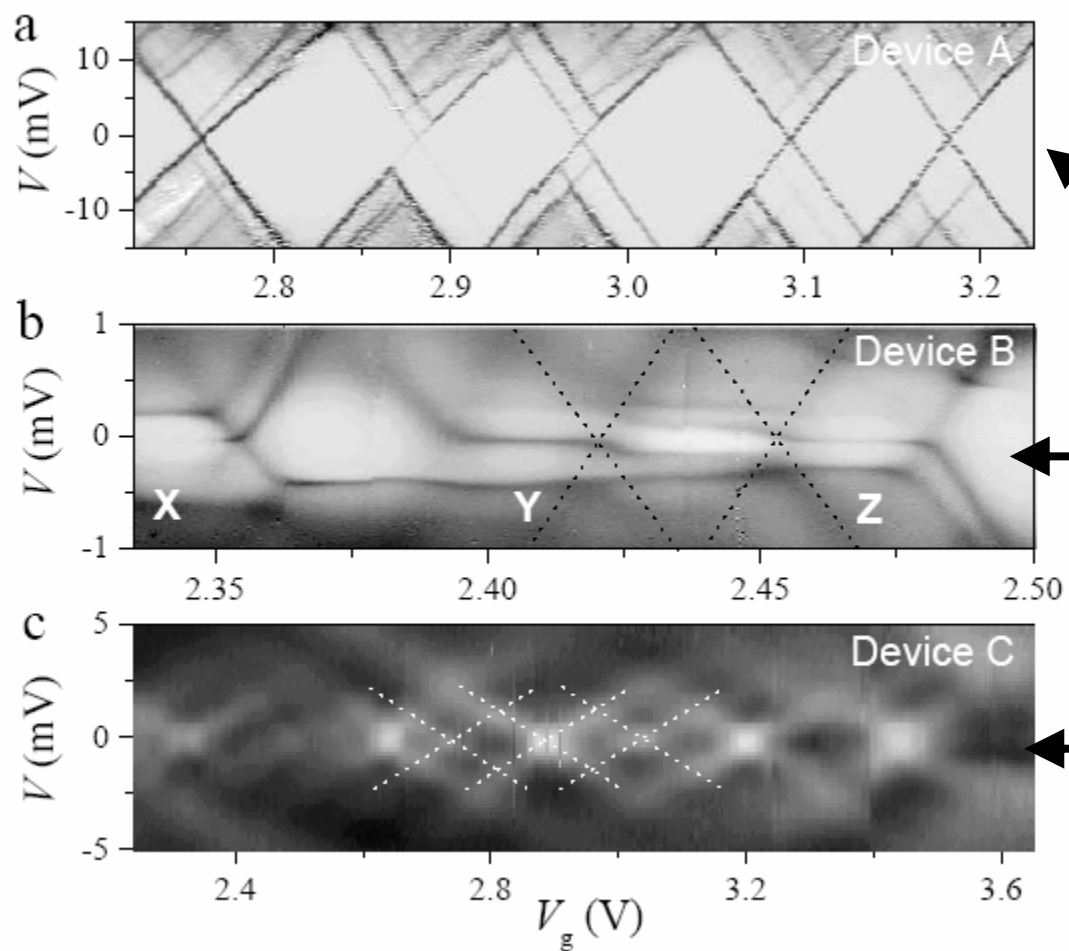
ε_0  H

Γ  Γ, Σ

N  $Tr(\rho)$

U_{SCF}  U_{SCF}

Strong vs. weak confinement



CB (T = 75 mK, P_C = 0.15)

Kondo features at V=0, (T = 75 mK, P_C = 0.6)

Interference patterns (T = 1.2 K, P_C = 0.9)

$$G_{\max} = 4 e^2 / h$$

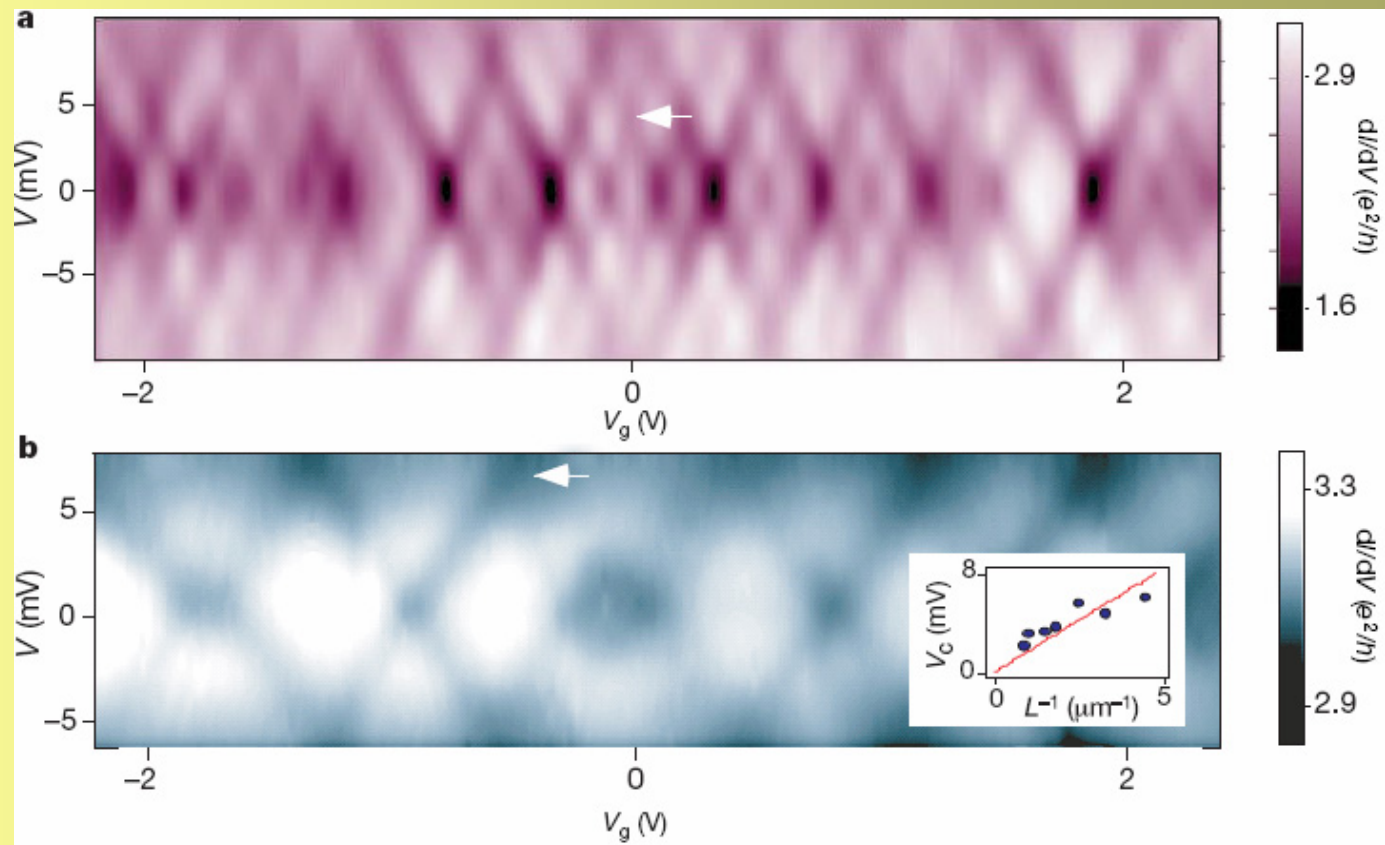
$$G_{RT} = G_{\max} P_C / (2 - P_C)$$

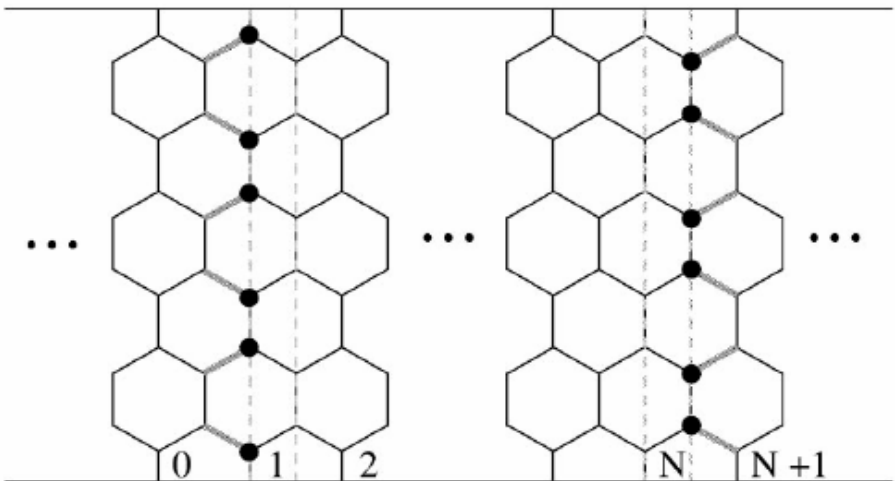
$$0 \leq P_C \leq 1 \text{ (transmission probability)}$$

High transparency contacts (quasi ballistic regime)

Liang, Nature 2001

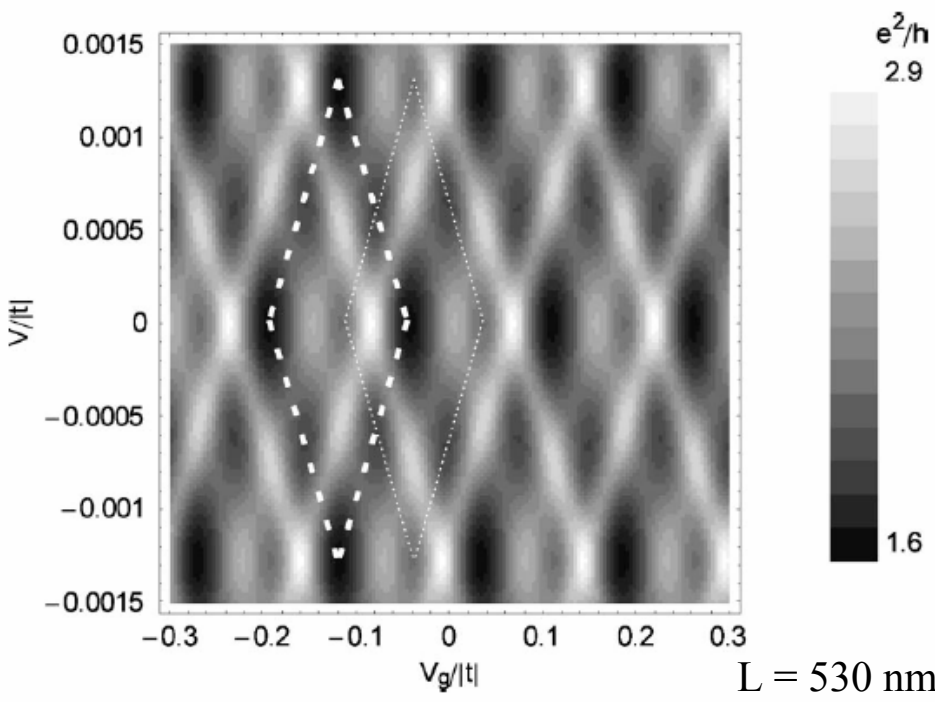
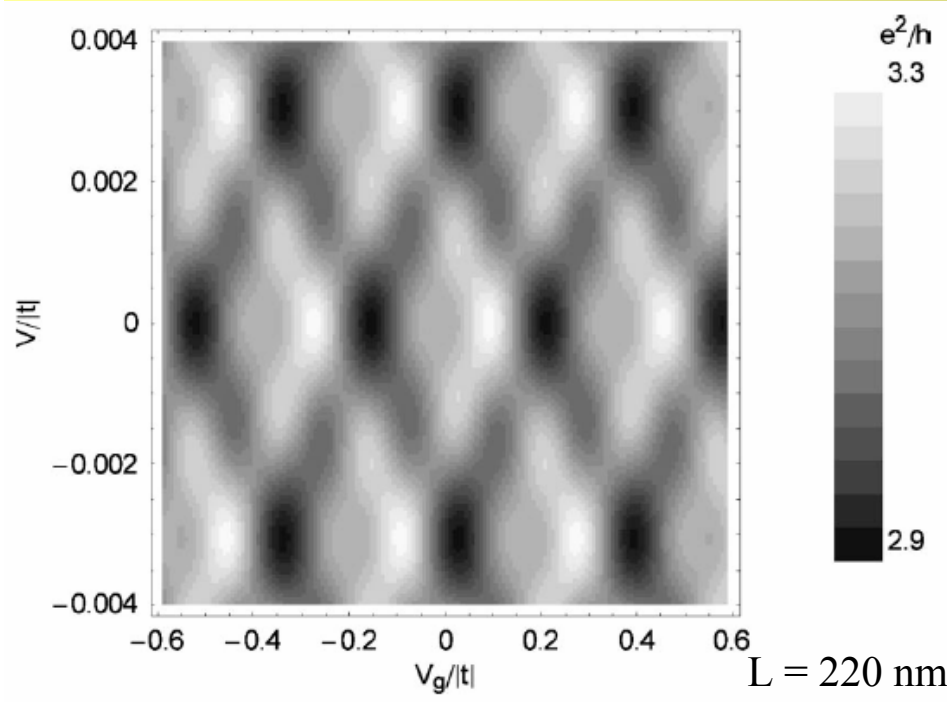
$L = 530 \text{ nm}$





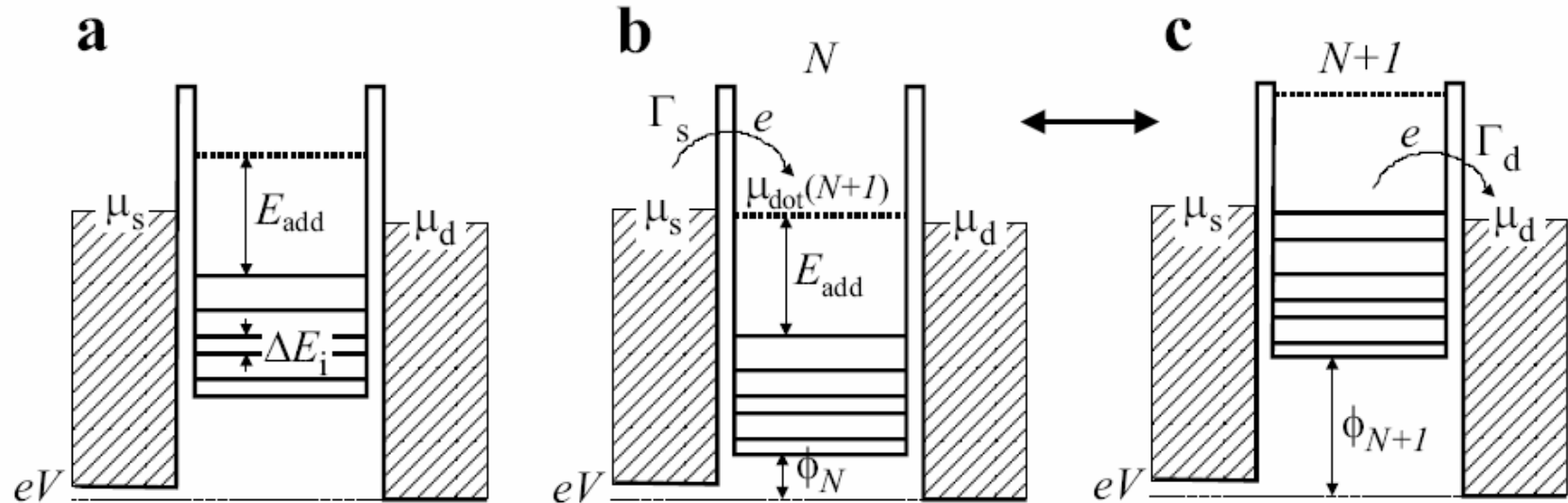
Krompiewski, et al.
PRB 2002

$$\frac{\partial I(V)}{\partial V} = \frac{e^2}{h} \left[T\left(E_F + \frac{eV}{2}, \Phi\right) + T\left(E_F - \frac{eV}{2}, \Phi\right) \right]$$



Coulomb Blockade

(Nygard 2000)



$$F(N) = U(N) + \sum_{i=1}^N E_i$$

$$U(N) = \frac{Q_{\text{ex}}^2}{2C} = \frac{(-e(N - N_0) - C_g V_g)^2}{2C}$$

$$\mu_{\text{dot}}(N) = F(N) - F(N - 1) = \underbrace{\frac{e^2}{C} \left((N - N_0) - \frac{1}{2} \right)}_{\text{Addition energy}} - e \frac{C_g}{C} V_g + E_N$$

Addition energy

ϕ_N

$$E_{\text{add}} = \mu_{\text{dot}}(N + 1) - \mu_{\text{dot}}(N) = \underbrace{\frac{e^2}{C}}_{\text{---}} + (E_{N+1} - E_N) = E_c + \Delta E_{N+1}$$

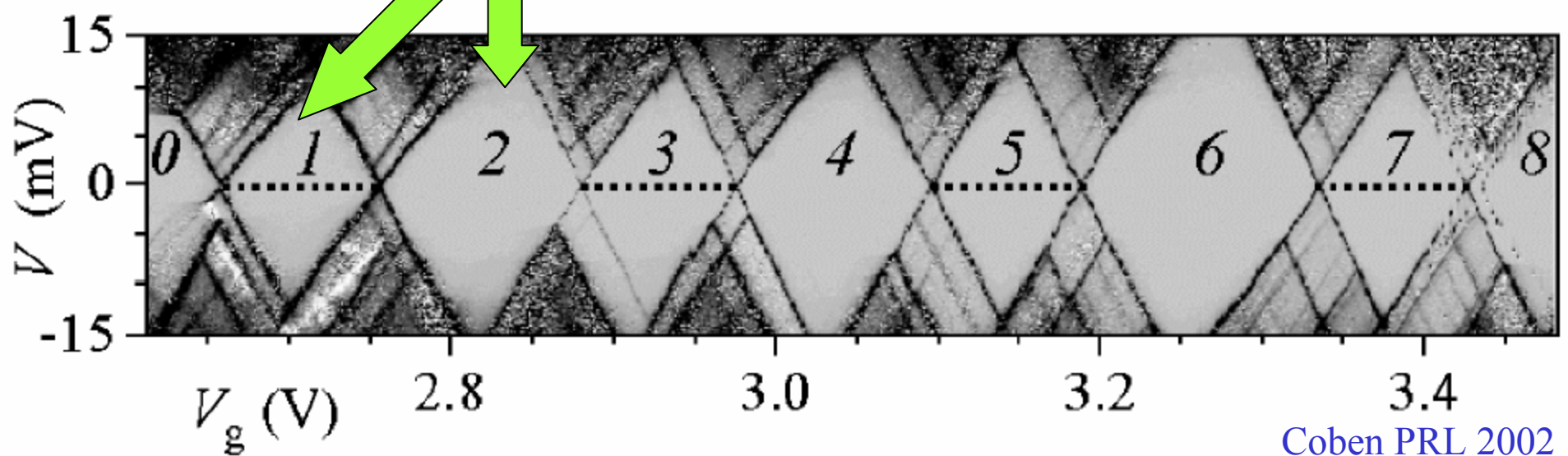
The rules of thumb

$$E_C = e^2/C \sim e^2/(\epsilon_0 \epsilon L) \sim 5 \text{ meV}/L [\mu\text{m}], \quad (\epsilon = 4 \text{ for SiO}_2)$$

$$\Delta E = (dE/dk) (\Delta k/2) = \hbar v_F (\pi/2L) \sim 1 \text{ meV}/L[\mu\text{m}]$$

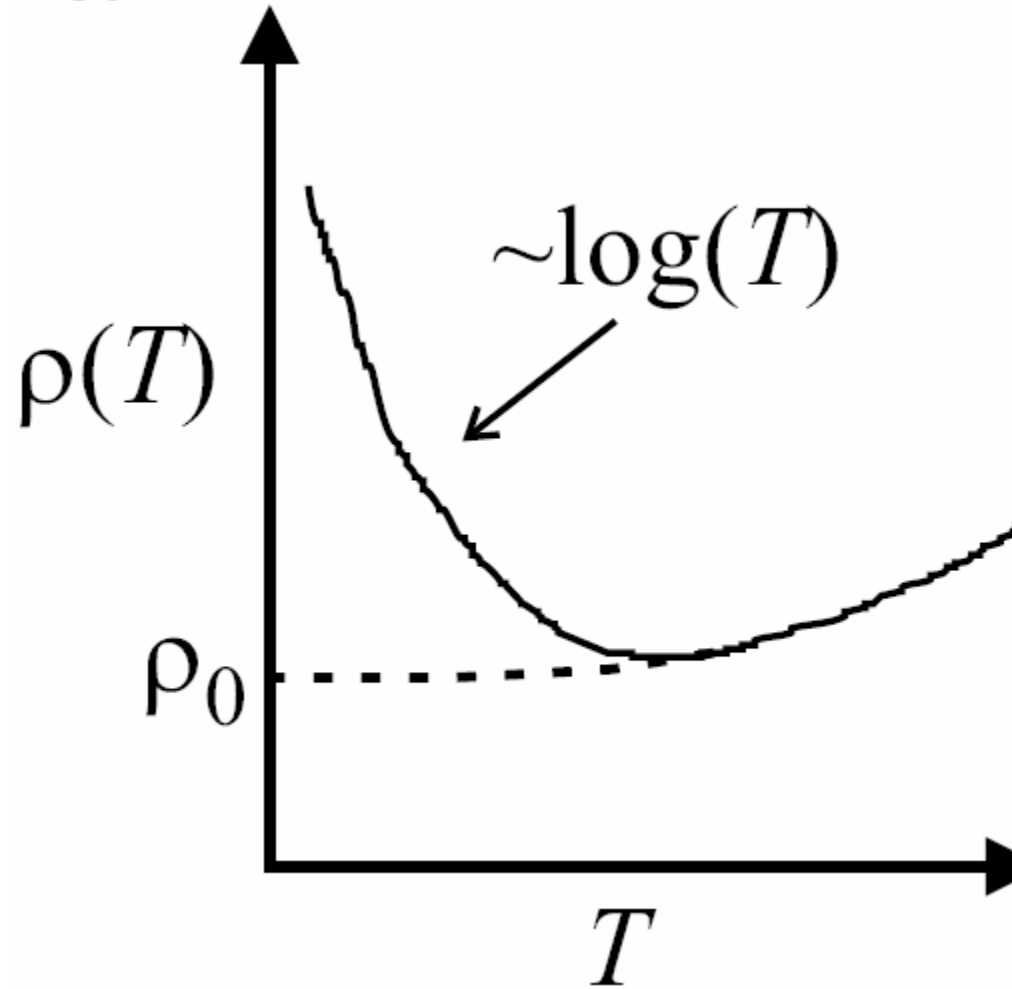
Note that $E_C/\Delta E \sim 5$ is L- independent

Even- odd shell filling
 $(E_C, E_C + \Delta E, E_C, E_C + \Delta E, \dots)$



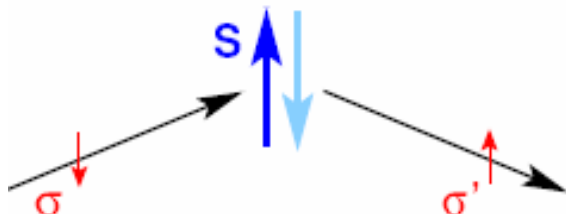
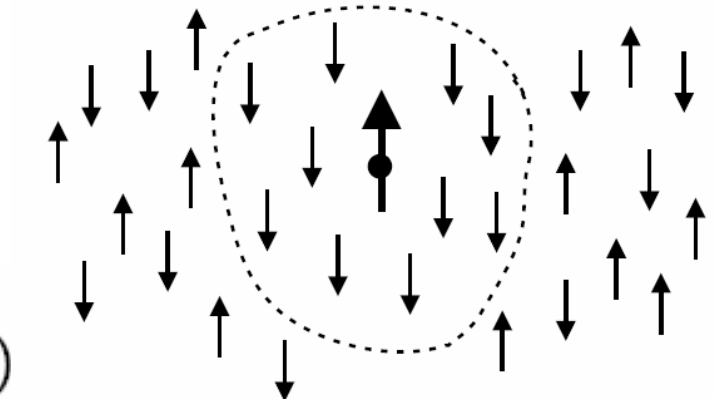
Coben PRL 2002

Kondo effect (1964)



$$\rho(T) \sim a T^5 - b \log(T)$$

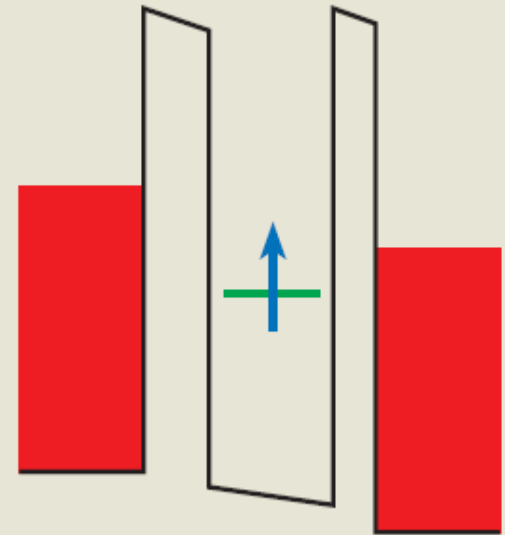
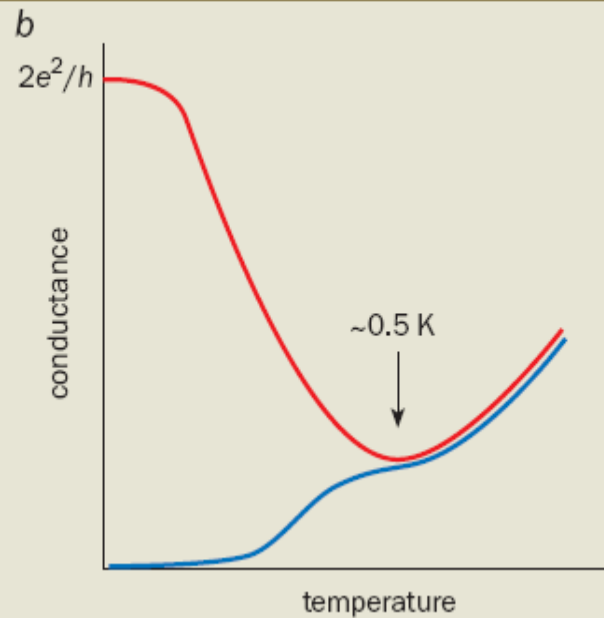
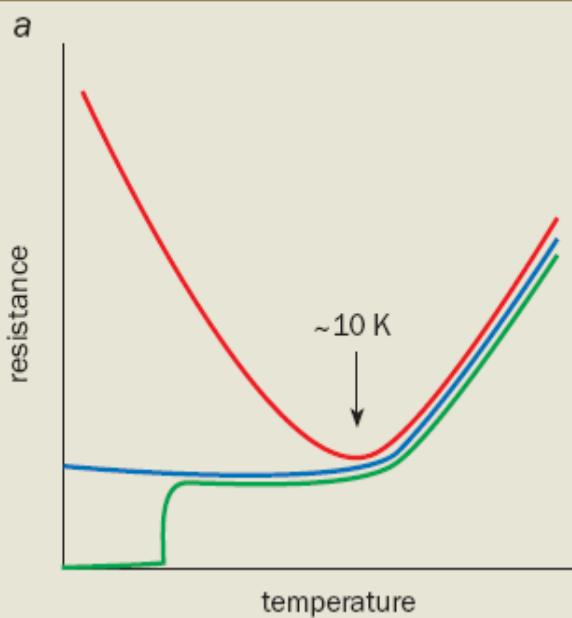
$$J (\vec{S} \cdot \vec{\sigma})$$



Resonant spin scattering
at the Fermi energy

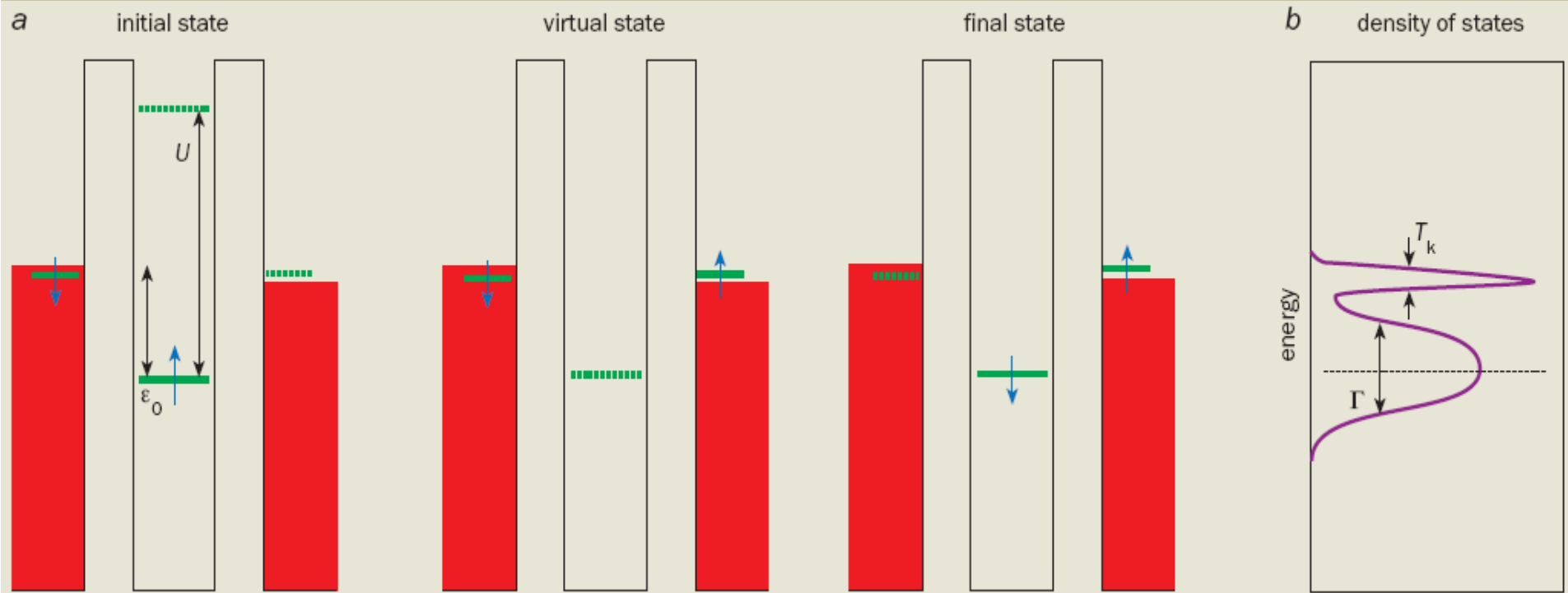
e.g. Au + 0.1% Fe
 $T_K \sim$ a few K

1 The Kondo effect in metals and in quantum dots

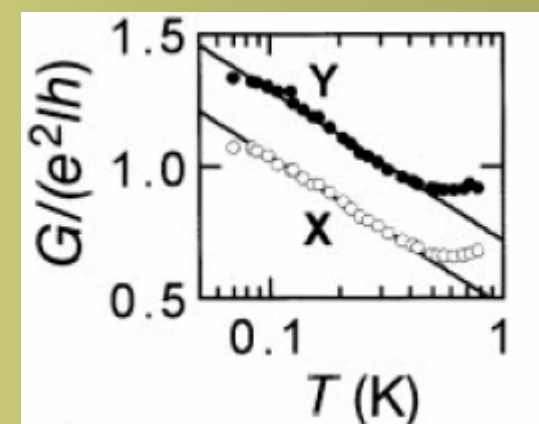
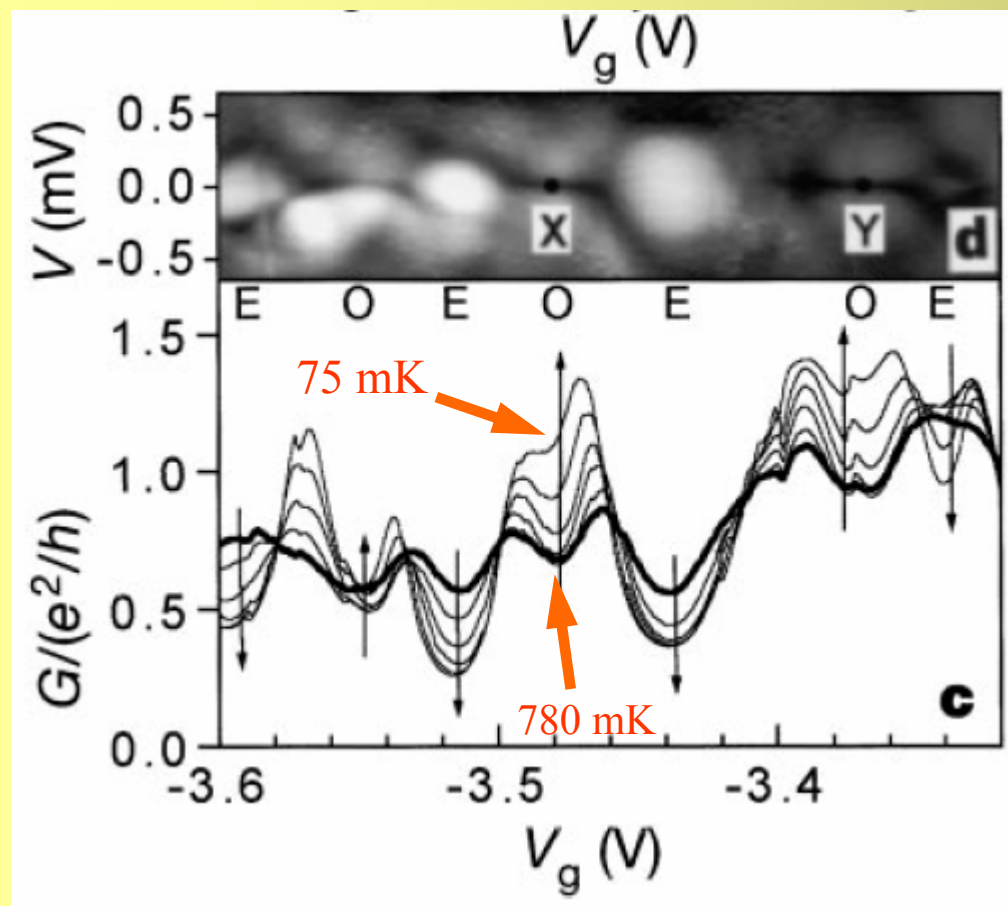


(a) As the temperature of a metal is lowered, its resistance decreases until it saturates at some residual value (blue). However, in metals that contain a small fraction of magnetic impurities, such as cobalt-in-copper systems, the resistance increases at low temperatures due to the Kondo effect (red). (b) A system that has a localized spin embedded between metal leads can be created artificially in a semiconductor quantum-dot device containing a controllable number of electrons. If the number of electrons confined in the dot is odd, then the conductance increases due to the Kondo effect at low temperature (red). In contrast, the Kondo effect does not occur when the dot contains an even number of electrons and the total spin adds up to zero. In this case, the conductance decreases with temperature (blue).

2 Spin flips

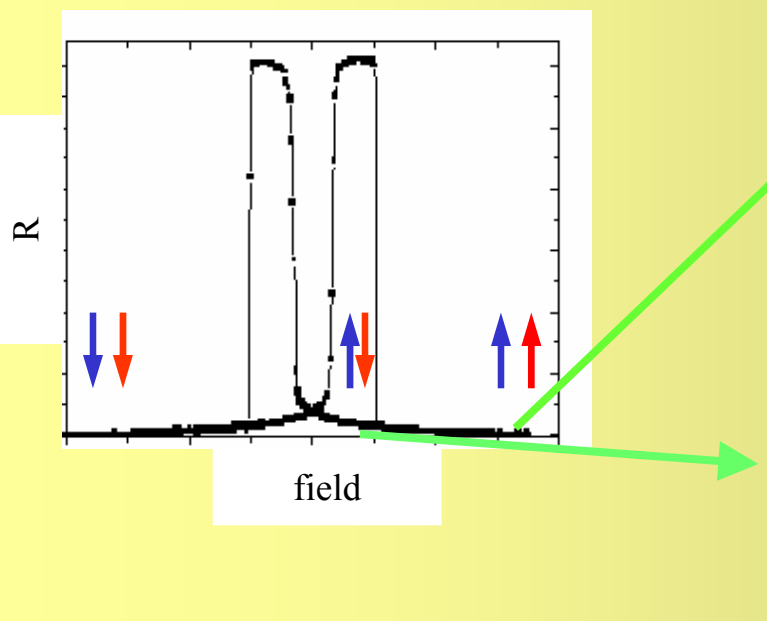
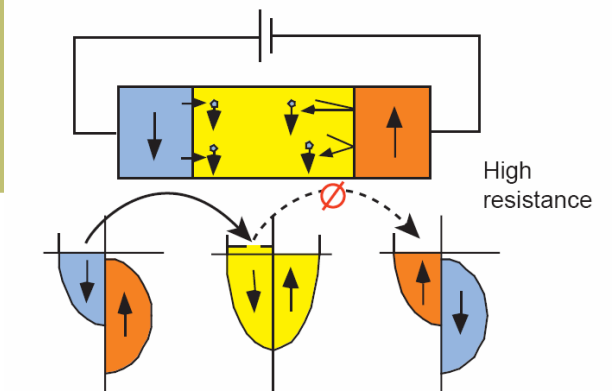
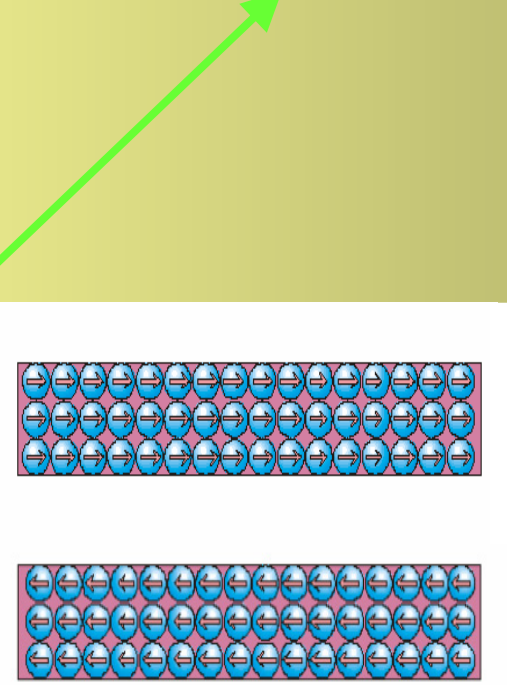
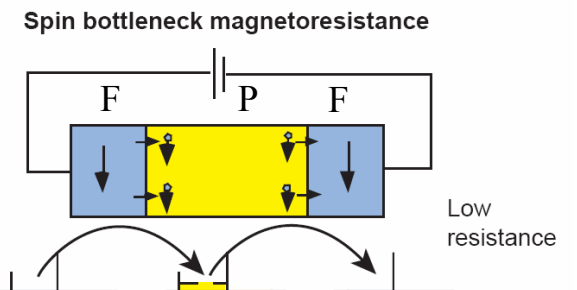
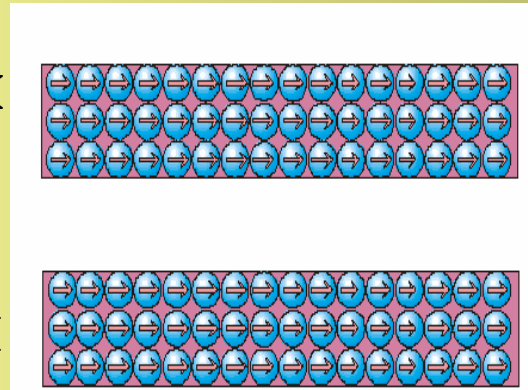
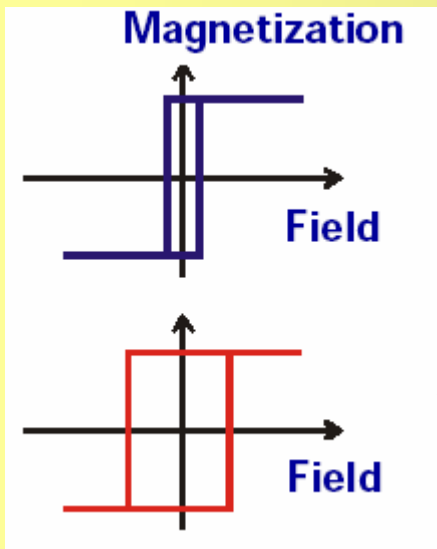


The Anderson model of a magnetic impurity assumes that it has just one electron level with energy ε_0 below the Fermi energy of the metal (red). This level is occupied by one spin-up electron (blue). Adding another electron is prohibited by the Coulomb energy, U , while it would cost at least $|\varepsilon_0|$ to remove the electron. Being a quantum particle, the spin-up electron may tunnel out of the impurity site to briefly occupy a classically forbidden “virtual state” outside the impurity, and then be replaced by an electron from the metal. This can effectively “flip” the spin of the impurity. (b) Many such events combine to produce the Kondo effect, which leads to the appearance of an extra resonance at the Fermi energy.



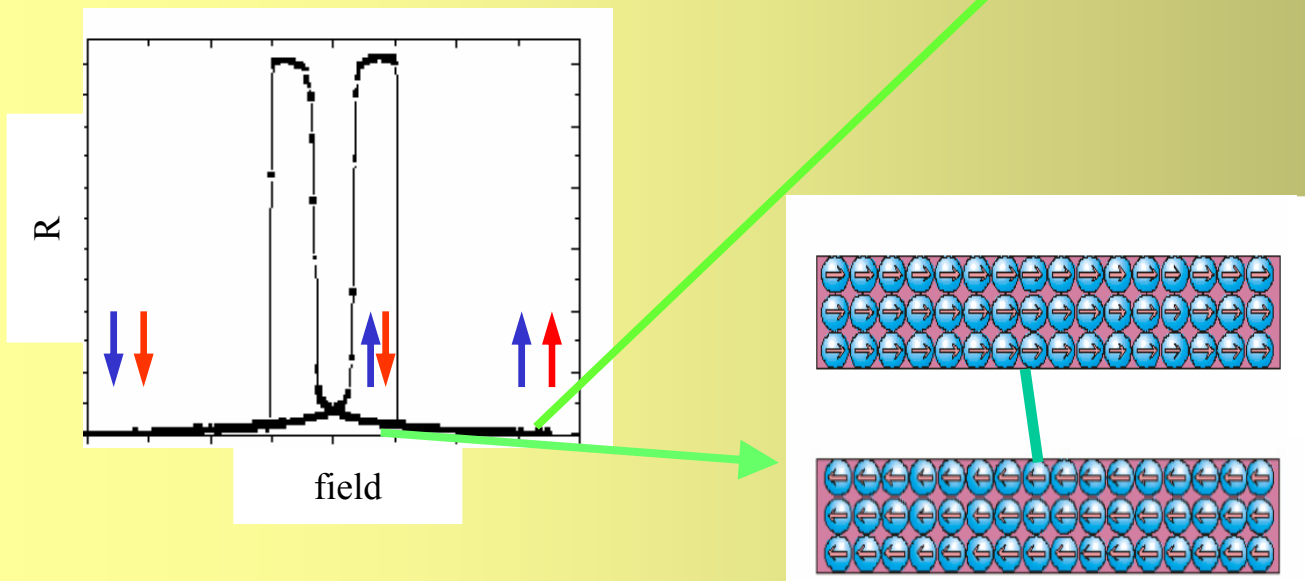
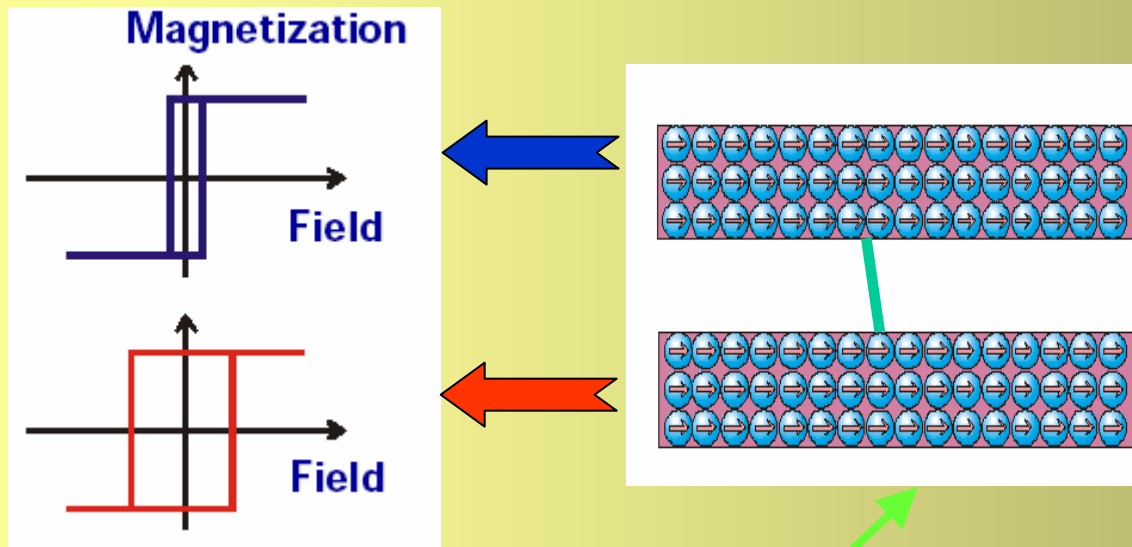
In „Odd“ regions G increases logarithmically with decreasing T

GMR



Prinz

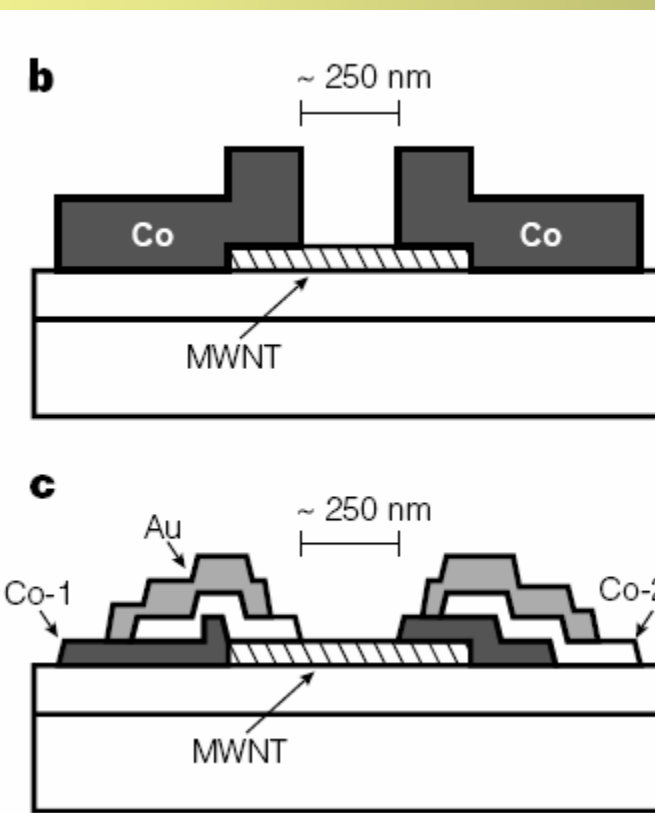
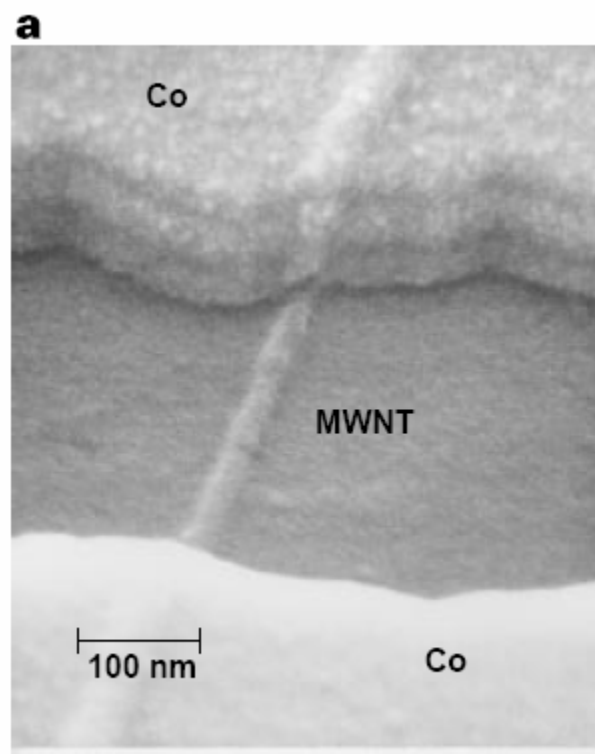
GMR



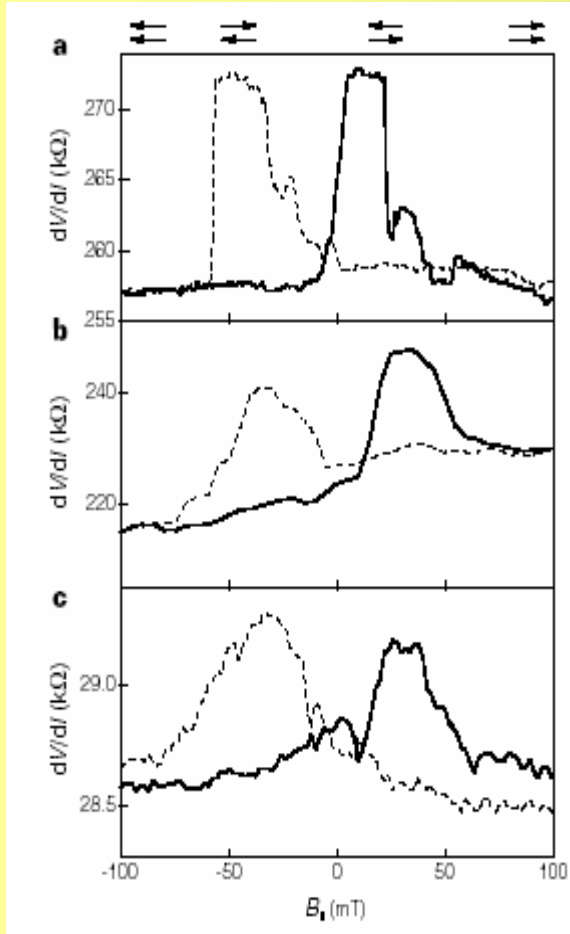
K.Tsukagoshi, B. Alphenaar,..

Nature'1999

GMR ca. 9%, MWCNT + Co contacts



A single multi-walled carbon nanotube electrically contacted by ferromagnetic Co.
a, Scanning electron microscope image of the device, near the Co/MWNT junction.
b (c), Schematic diagram of the device.



$$\text{GMR} = \Delta R/R_{AP} = (R_{PA} - R_{AP})/R_{AP}$$

$$= 2 P_1 P_2 / (1 + P_1 P_2)$$

For Co P = 34%

expected GMR_{Julliere} = 21 %

measured GMR_{exp} = 9% → P_{reduced}

Spin-polarization reduces as:

$$\exp(-L/L_s)$$

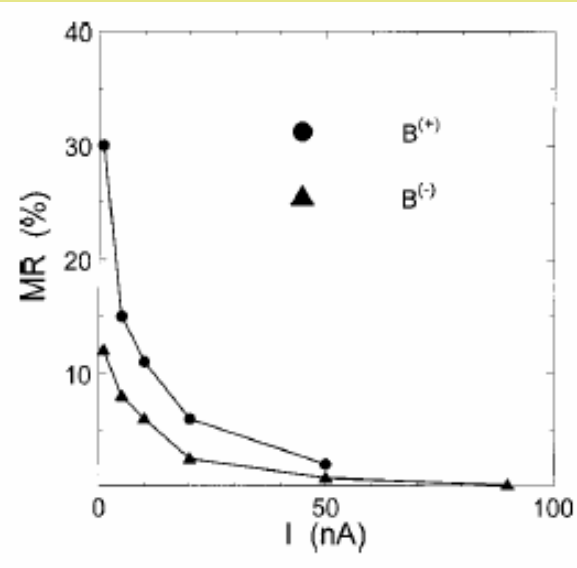
For L = 250 nm, one finds

$$L_s \sim 130 \text{ nm}$$

Experiments

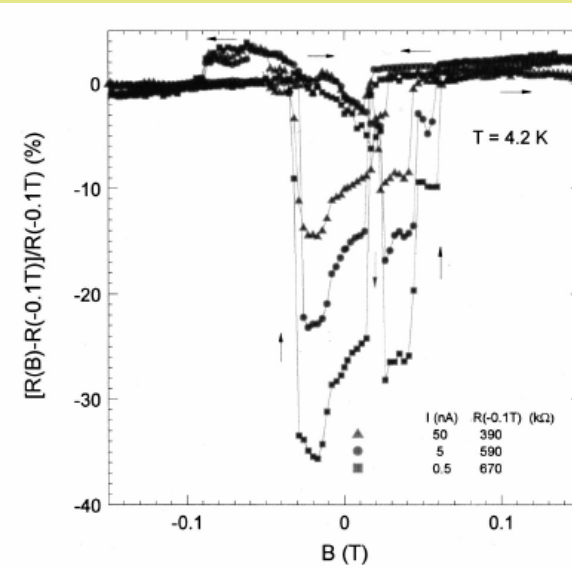
B. Zhao et al.,
Appl. Phys. Lett.'2002
GMR 10% – 30%

MWCNT + Co contacts



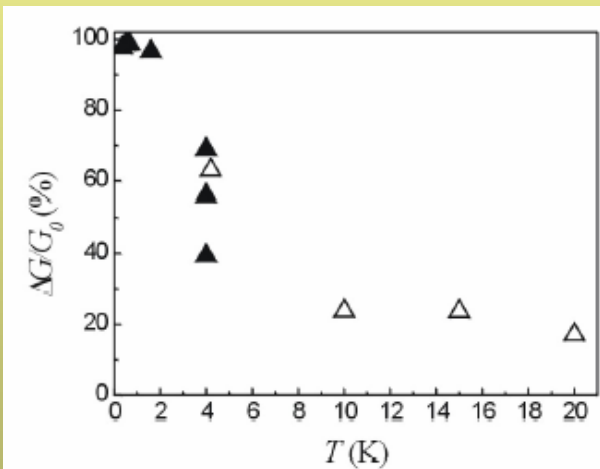
B. Zhao et al.,
J.Appl. Phys.'2002
GMR < 0

MWCNT + Co contacts

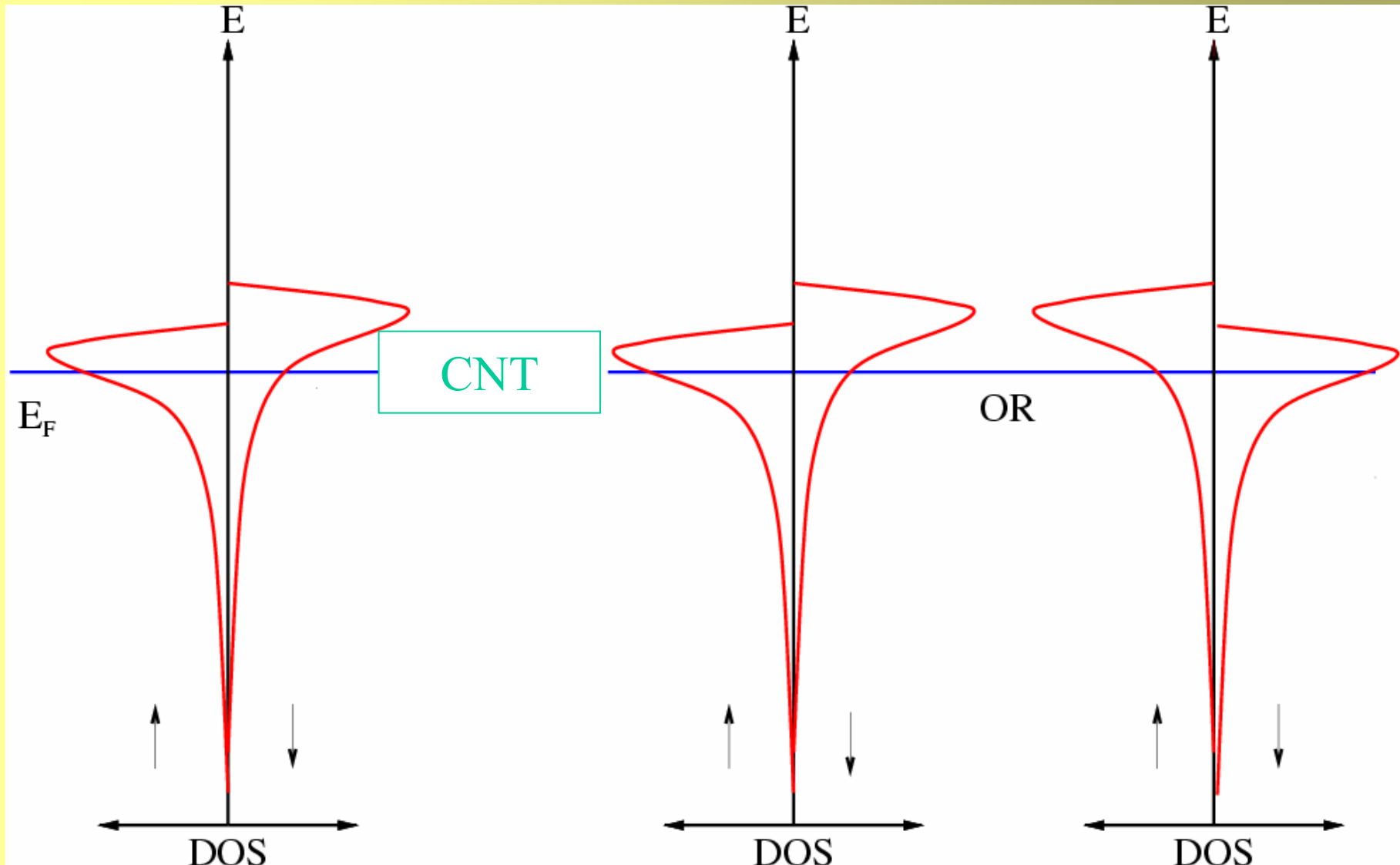


A. Jensen, J. Nygard,...
World Scientific'2002
GMR up to 100%

SWCNT + Fe contacts



Ferromagnetically contacted carbon nanotube



Methodology

$$H = \sum_{i,j,\sigma} t_{i,j} |\sigma, i\rangle\langle j, \sigma| + \sum_{i,\sigma} \epsilon_{i,\sigma} |\sigma, i\rangle\langle i, \sigma|,$$

$$\begin{pmatrix} E_\sigma - H_L^\sigma & V_{LC} & 0 \\ V_{LC}^\dagger & E_\sigma - H_C^\sigma & V_{CR} \\ 0 & V_{CR}^\dagger & E_\sigma - H_R^\sigma \end{pmatrix} \hat{\mathcal{G}}_\sigma = \hat{1},$$

$$G_\sigma \equiv \hat{\mathcal{G}}_C^\sigma = (\hat{1} E_\sigma - H_C^\sigma - \Sigma_{L,\sigma} - \Sigma_{R,\sigma})^{-1},$$

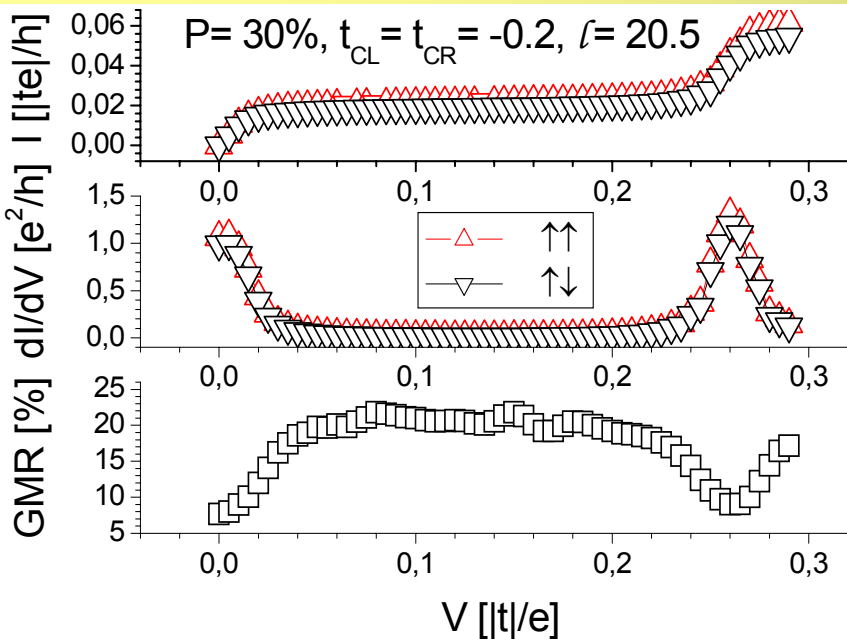
$$n_\sigma = \frac{1}{2\pi} \int dE G_\sigma (f_{L,\sigma} \Gamma_{L,\sigma} + f_{R,\sigma} \Gamma_{R,\sigma}) G_\sigma^\dagger,$$

$$I_\sigma = \frac{e}{h} \int_{-\infty}^{\infty} dE (f_{L,\sigma} - f_{R,\sigma}) \text{Tr}[\Gamma_{L,\sigma} G_\sigma \Gamma_{R,\sigma} G_\sigma^\dagger],$$

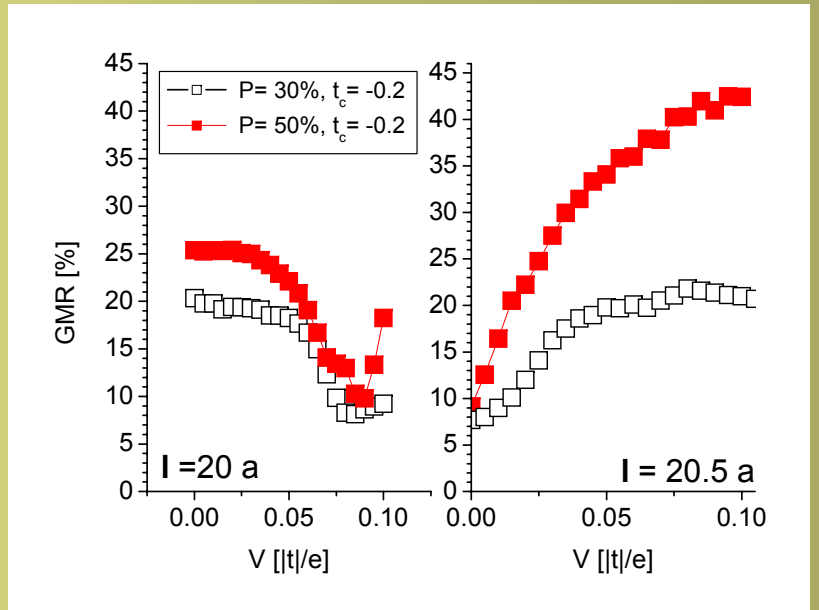
where

$$\Gamma_{\alpha,\sigma} = i(\Sigma_{\alpha,\sigma} - \Sigma_{\alpha,\sigma}^\dagger), \quad \Sigma_{\alpha,\sigma} = V_{C,\alpha} g_{\alpha,\sigma} V_{C,\alpha}^\dagger \quad f_{\alpha,\sigma} = \left(1 + \exp\left[\frac{E_\sigma - \mu_\alpha}{k_B T}\right]\right)^{-1}$$

and $\alpha = L, R$ stand for left- and right-hand sides, σ denotes the spin and $\mu_\alpha = E_F \pm eV/2$.

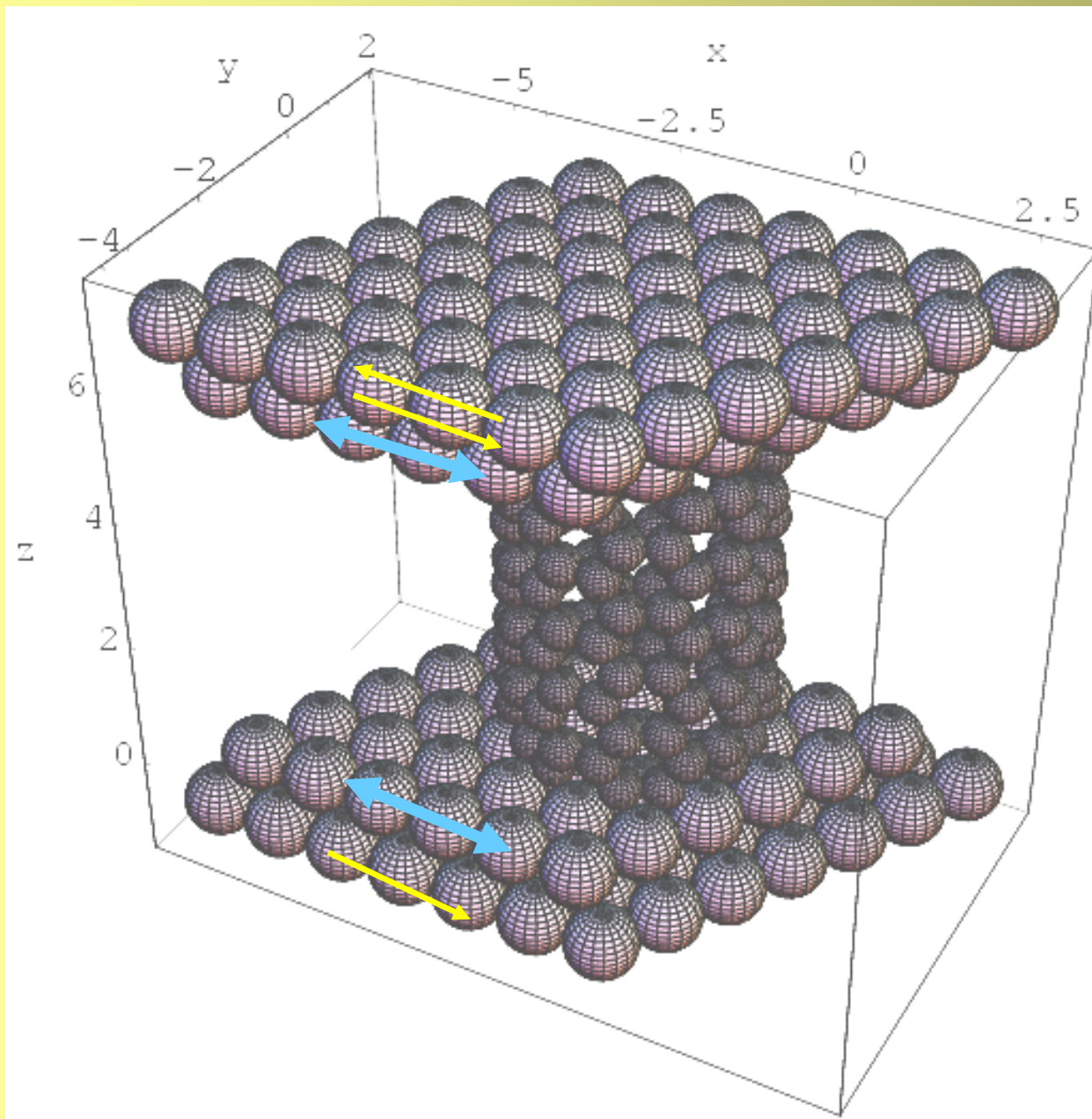


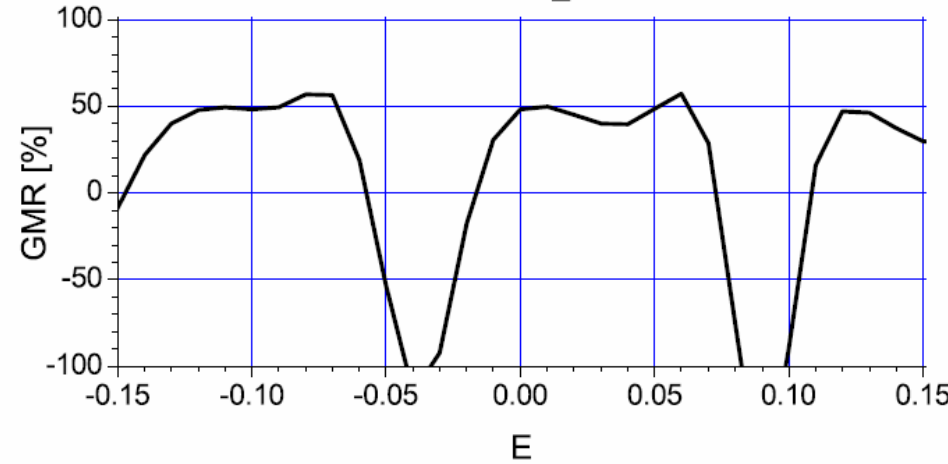
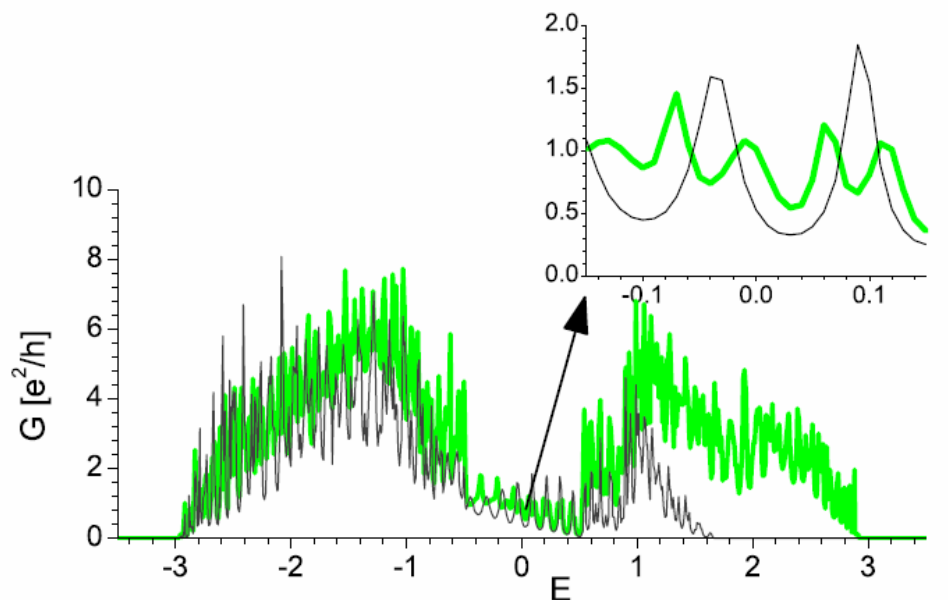
SWCNT length = 20.5 a
 („on-resonance”)



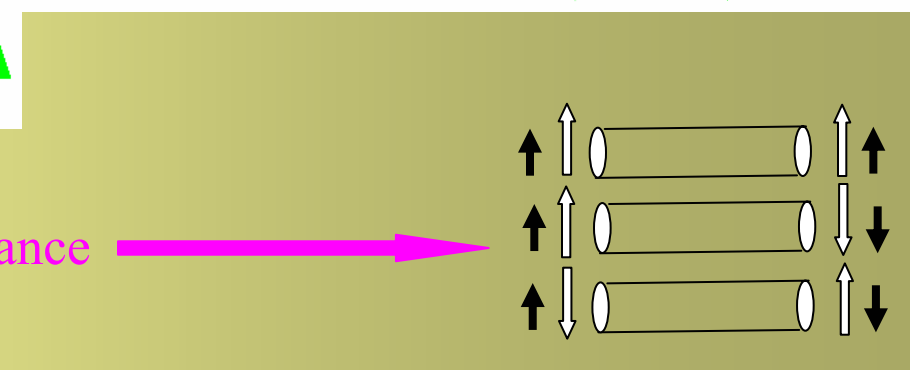
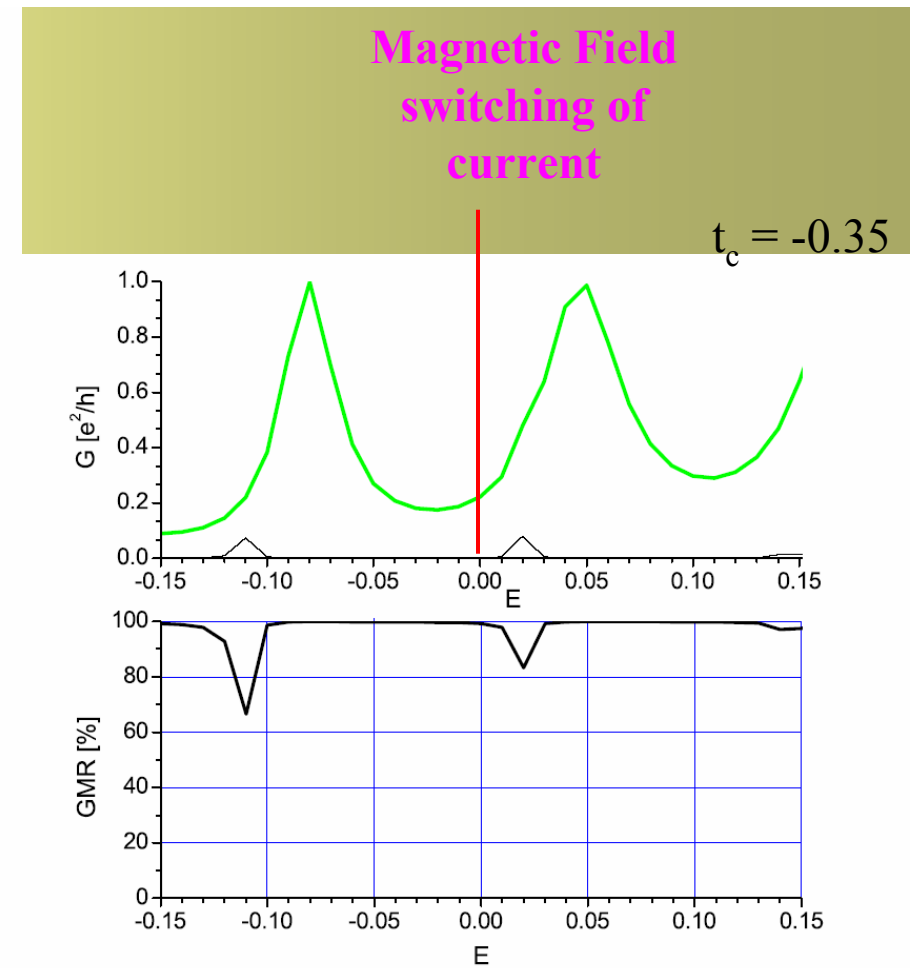
GMR vs. V for different SWCNT lengths (l) and surface magnetization (P) of electrodes

Modeling a spin-selective interface

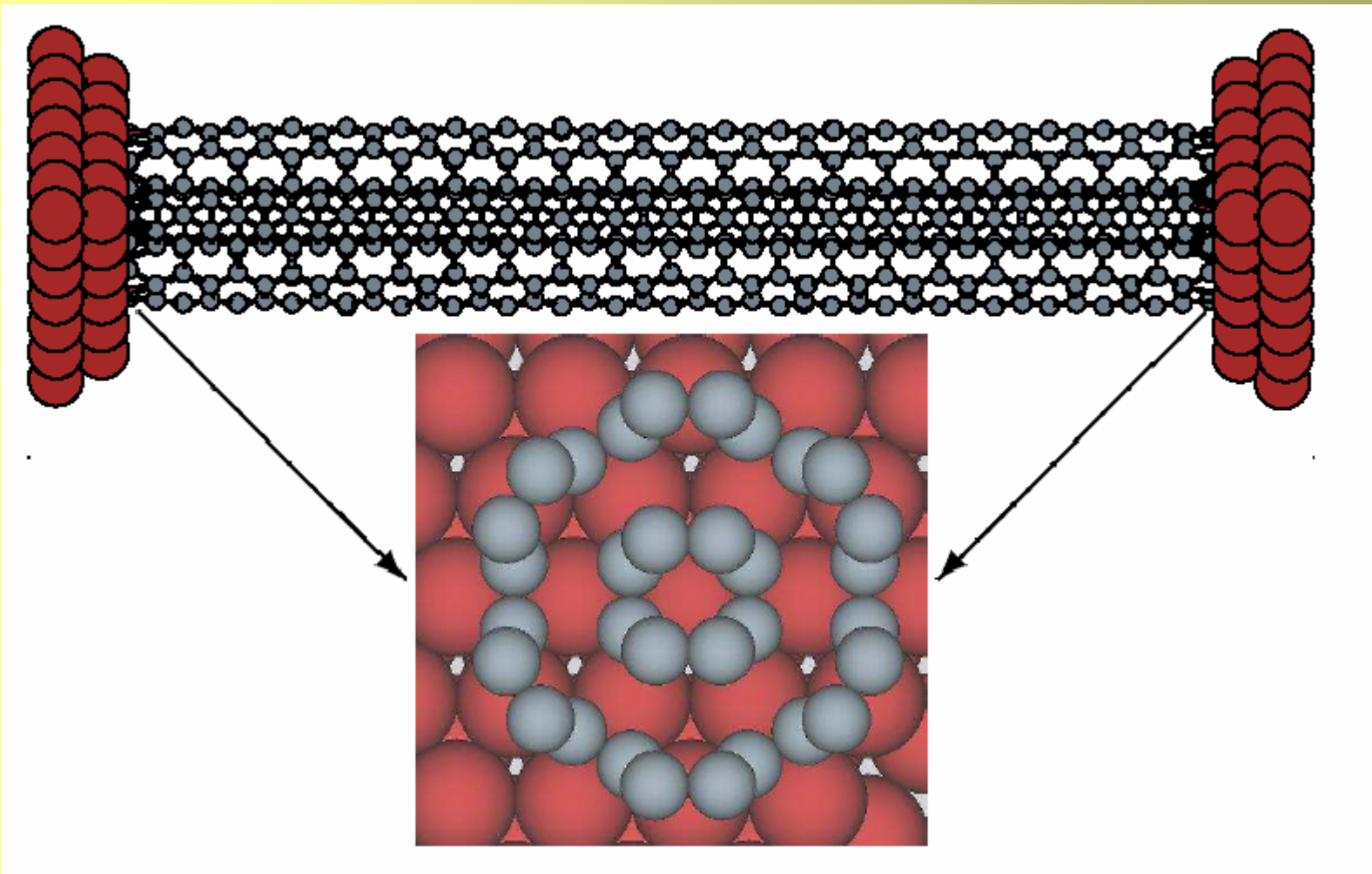




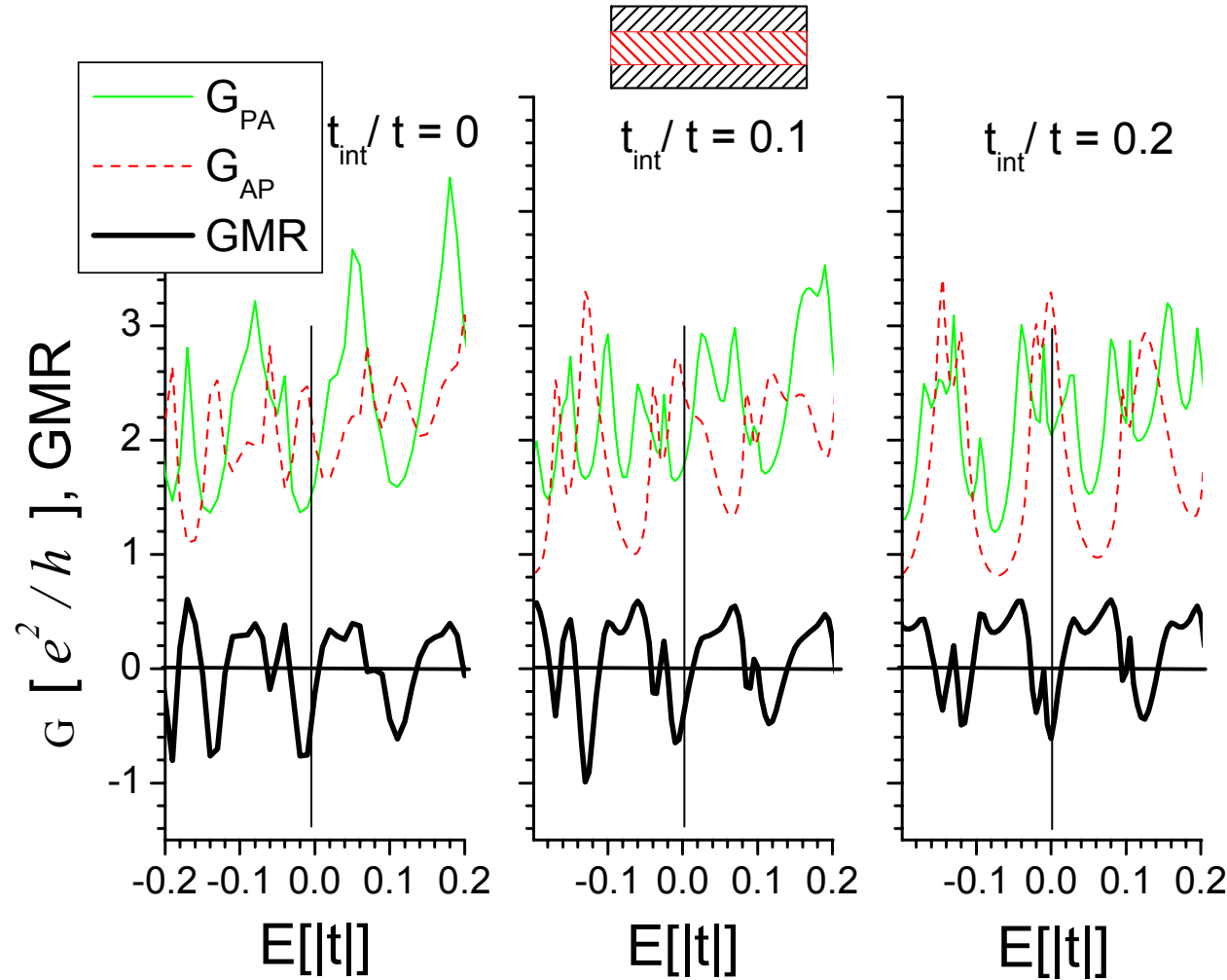
3-valued conductance



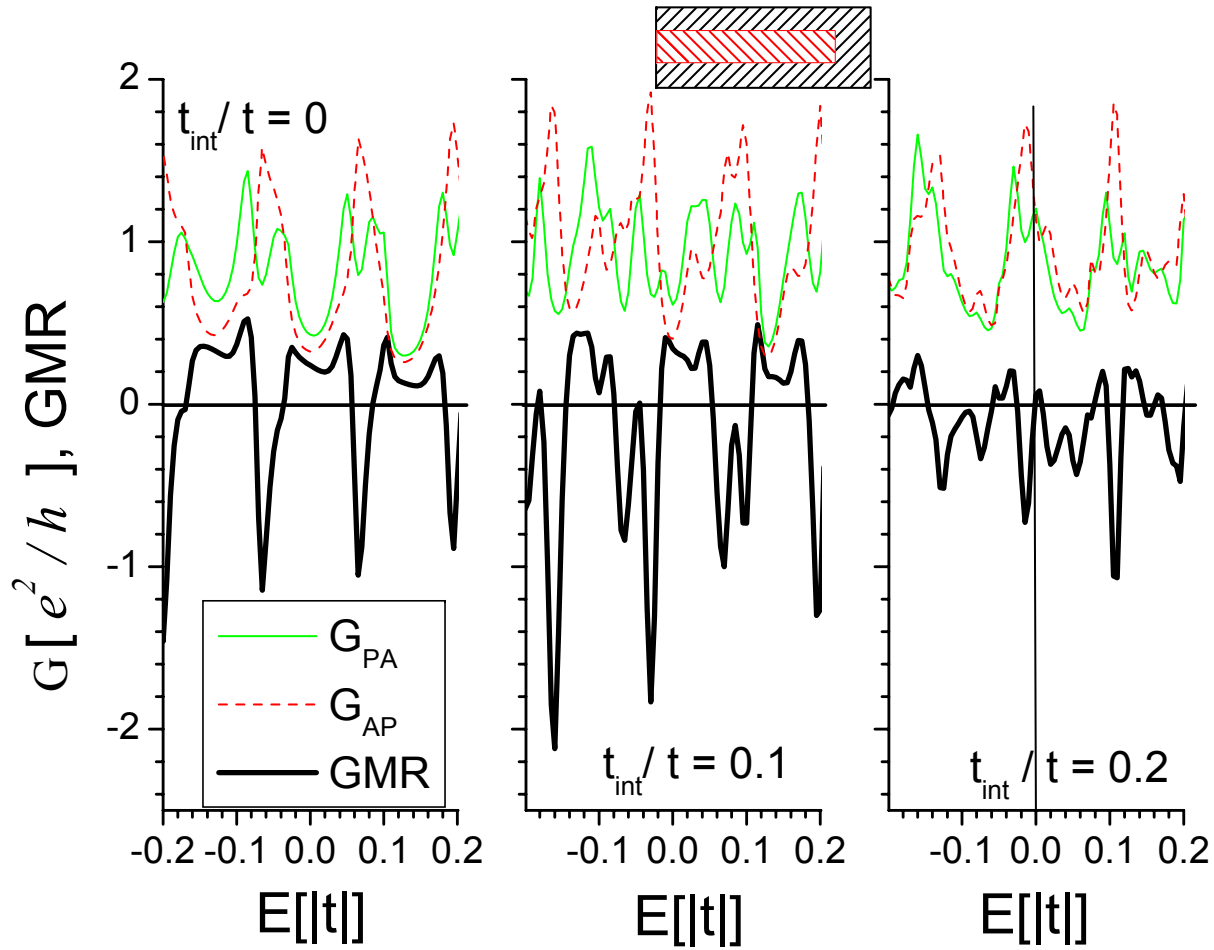
Minimal geometrical model of the DWCNT



View of the (2,2)@(6,6) carbon nanotube sandwiched between two fcc(111) leads and detail of the contact region. What is shown consists of a few ferromagnetic electrode atoms with the nanotube forming the so-called extended molecule. The other parts of the electrodes (not shown) are infinite in all the directions.

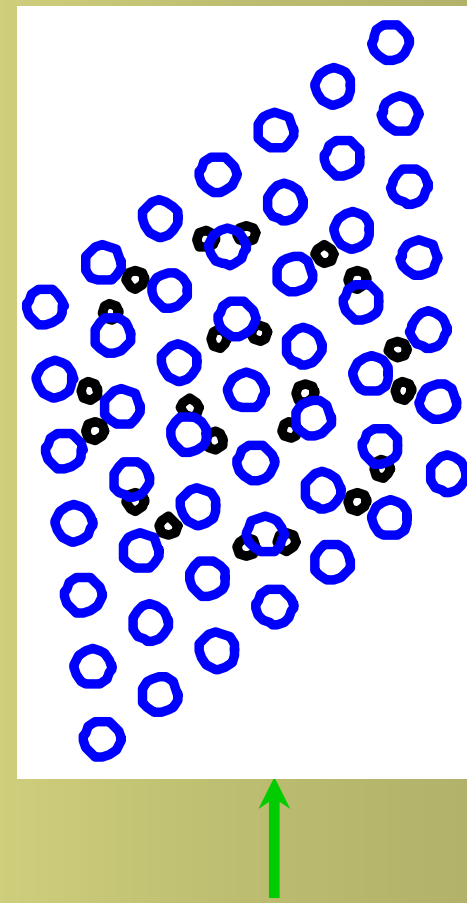
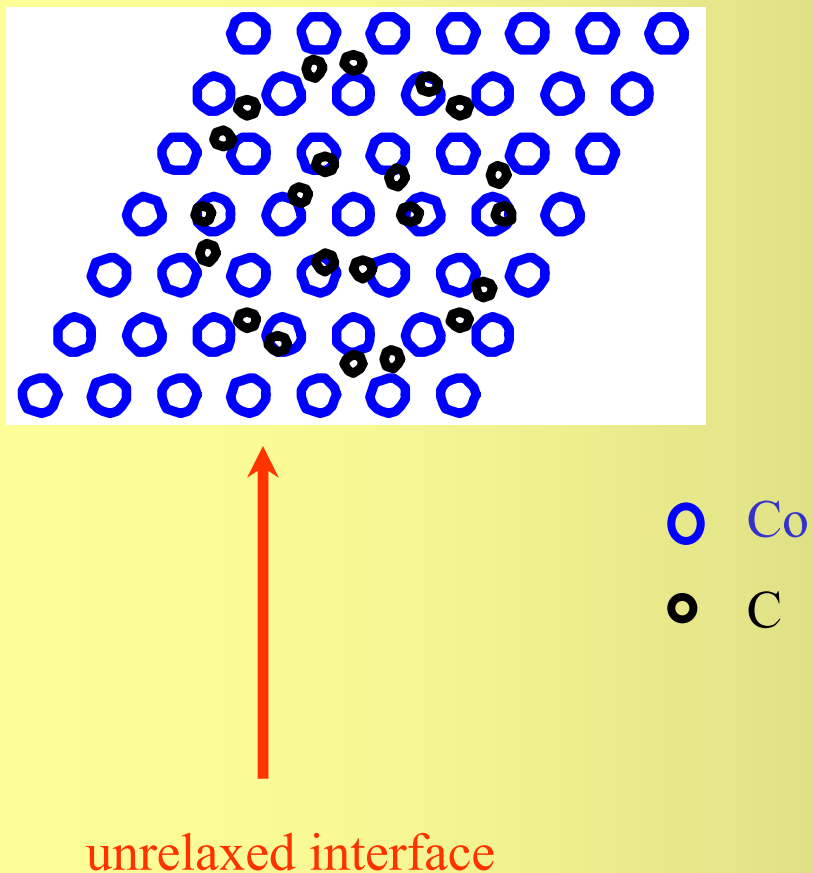


The total conductance for the parallel (PA) and antiparallel (AP) alignments, as well as the GMR vs. energy. The outer nanotube length equals that of the inner one ($L_{out} = L_{in} = 41$ carbon rings), the Fermi energy is equal to $E_F = 0$. Left panel: there are no inter-wall interactions ($t_{int}=0$). Middle and right panels: the inter-wall interactions are included.



Unlike in the previous figure, here the inner tube is out of contact to the right electrode. A drastic drop in the conductance (at E_F), accompanied by a positive GMR, takes place. No inter-wall interactions (left panel), and $t_{\text{int}}/t = 0.1$ and 0.2 (middle and right panels, respectively).

The present approach may be regarded as a reference for further generalizations. The diameters and the number of walls forming the MWCNT may be easily increased and the respective stable positions of the interface atoms can be readily determined by a simple relaxation procedure involving just a few variation parameters (displacements and rotations).



relaxed under the van der Waals potential

More realistic parameterization
[S. Roche et al., (2001)]

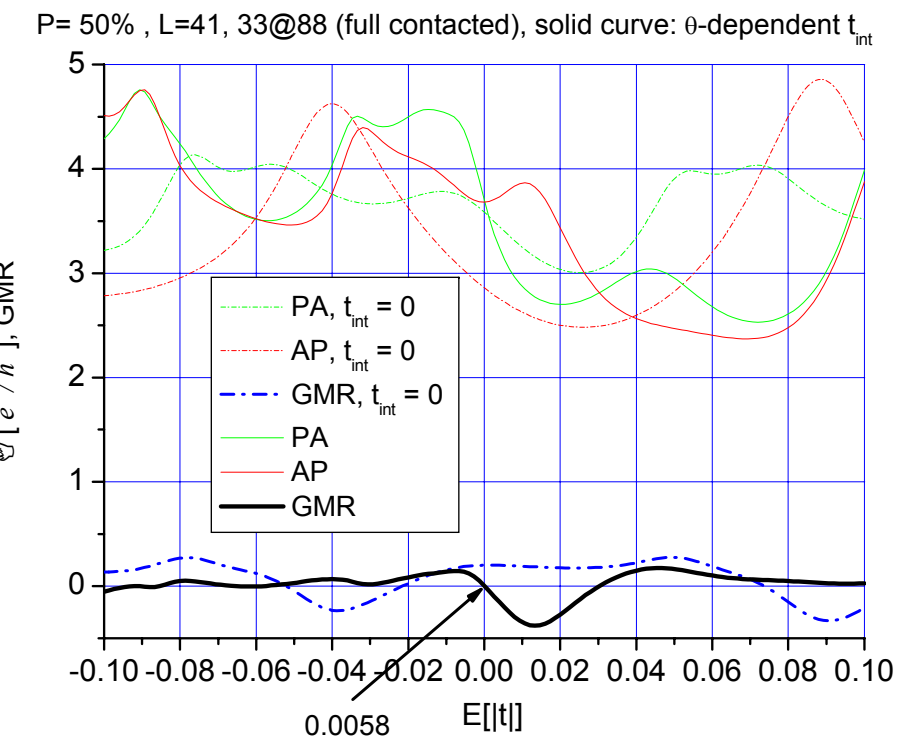
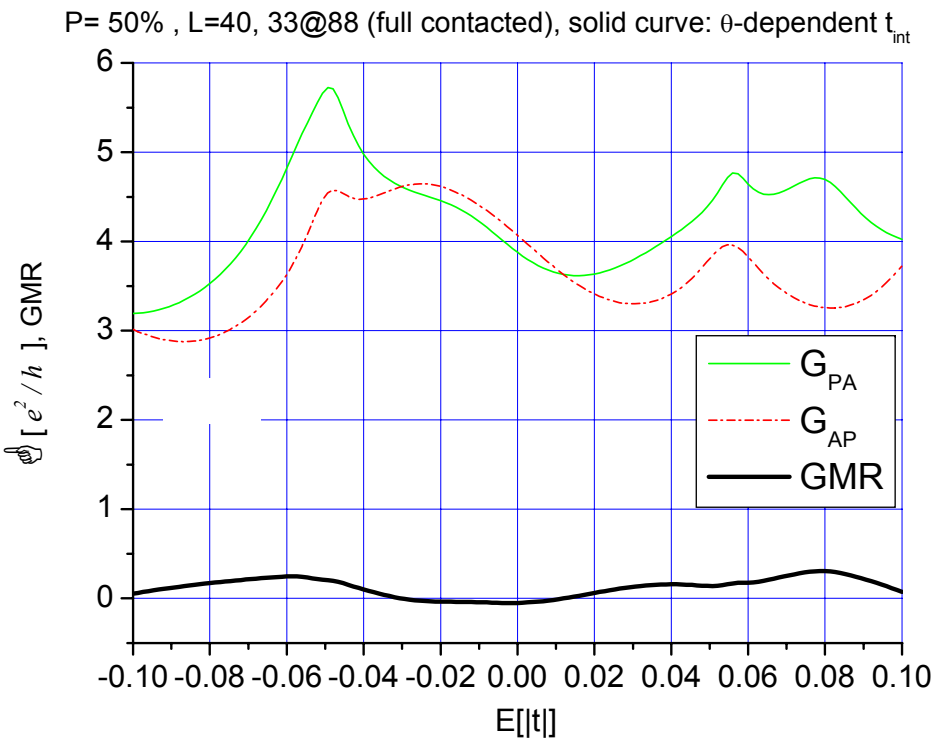
$$t_{\text{inter-wall}}(i,j) = -(t/8) \cos(\theta_{ij}) \exp [(d_{ij} - a)/\delta]$$

θ angle between the π orbitals

d relative distance

$$\delta = 0.45 \text{ \AA}$$

$$a = 3.34 \text{ \AA}$$



G

CONCLUSIONS

1. Toy model (Datta) captures essential physics
2. Depending on the interface (increasing contact transparencies): Coulomb, Kondo and ballistic regimes
3. GMR:
 - CNT-length dependent (on- vs. off-resonance devices),
 - strongly enhanced if interfaces are spin-selective,
 - critically dependent on whether or not the inner tubes of the MWCNTs are contacted to the electrodes,
 - non-monotonically dependent on the inter-wall coupling strength.